

CASE FILE
COPY

NATIONAL ADVISORY COMMITTEE
FOR AERONAUTICS

TECHNICAL NOTE

No. 1850

THE YAWING MOMENT DUE TO SIDESLIP OF TRIANGULAR,
TRAPEZOIDAL, AND RELATED PLAN FORMS IN
SUPERSONIC FLOW

By Arthur L. Jones and Alberta Alksne

Ames Aeronautical Laboratory
Moffett Field, Calif.



Washington

April 1949

NATIONAL ADVISORY COMMITTEE FOR AERONAUTICS

TECHNICAL NOTE NO. 1850

THE YAWING MOMENT DUE TO SIDESLIP OF TRIANGULAR,
TRAPEZOIDAL, AND RELATED PLAN FORMS IN
SUPERSONIC FLOW

By Arthur L. Jones and Alberta Alksne

SUMMARY

In this report expressions for the yawing moment due to sideslip in supersonic flow have been derived for a representative group of wing plan forms. The analysis was based on edge-suction theory as well as linearized potential theory and was applied to triangular, trapezoidal, rectangular, and swept-back plan forms without dihedral.

Values of the yawing-moment-due-to-sideslip derivative were computed for a number of typical plan forms with the assumption that the moment center was at the leading edge of the root chord. The triangular and swept-back plan forms possessed directional stability as long as their leading edges remained subsonic. The rectangular plan forms of low aspect ratio ($A \approx 2$) and the trapezoidal plan forms of moderately low aspect ratio ($A \approx 4$) were the only plan forms that possessed directional stability throughout the Mach number range investigated.

INTRODUCTION

The damping in roll and the rolling moment due to sideslip have been analyzed in references 1 and 2 for a group of wing plan forms representative of those usually proposed for flight at supersonic speeds. Stability derivatives based on these previous analyses are presented in references 1 and 2. Expressions for the yawing moment due to sideslip and the corresponding stability derivative are presented herein for the same group of plan forms.

The rolling moments given in references 1 and 2 were determined for a system of body axes. (See Symbols, Coefficients, and Axes and also fig. 1.) These rolling moments, moreover, can be applied as

well to the stability axes system if the angle of attack is kept very small. This condition is satisfied since the linearized compressible-flow theory requires that the angle of attack be kept small. The yawing moment relative to the stability axes, however, is appreciably different from the value of the yawing moment for the body axes. (See reference 3 for transformation formulas.) Since the stability axes are used most frequently in the calculation of dynamic stability, the yawing-moment expressions presented herein are derived with reference to the stability axes.

A complete theoretical value for the yawing moment due to sideslip must contain the effects of edge suction as well as the contributions of the normal forces. Since the pressures and velocities responsible for the edge-suction forces exceed the limitations of the linearized theory, the magnitudes of the suction component of the yawing moments presented herein probably should be more fully verified when experimental evidence or the results of an analytical approach more rigorous than the linearized theory become available.

Previous reports that include analysis of the yawing moment due to sideslip are reference 4 for triangular plan forms, reference 5 for a series of swept-back wings, and reference 6 for rectangular plan forms. These reports treat only infinitesimal angles of sideslip; whereas the present report treats finite angles in a range from zero to large values.

The plan forms investigated herein are shown in figures 2 and 3 and fit the following descriptions: (1) triangular with subsonic leading edges or with supersonic leading edges; (2) trapezoidal with all possible combinations of raked-in, raked-out, subsonic or supersonic tips; (3) rectangular; and (4) two swept-back plan forms with supersonic trailing edges developed from the triangular wings.

SYMBOLS, COEFFICIENTS, AND AXES

x, y, z	rectangular coordinates of wind axes (fig. 1)
ξ, η, ζ	rectangular coordinates of stability axes (fig. 1)
ξ', η', ζ'	rectangular coordinates of body axes (fig. 1)
$\xi'_{c.g.}$	location of the center of gravity or moment center aft of the leading edge of the root chord
V	free-stream velocity

b	span of wing measured normal to plane of symmetry
c_r	root chord of wing
l	over-all longitudinal length of swept-back wing
S	area of wing
A	aspect ratio $\left(\frac{b^2}{S} \right)$
ρ	air density in the free stream
q	free-stream dynamic pressure $\left(\frac{\rho v^2}{2} \right)$
T_L, T_R	total force due to suction on left or right edge (force is directed normal to edge)
N	yawing moment about ζ axis (positive for clockwise rotation in plan view)
N'	yawing moment about ζ' axis (positive for clockwise rotation in plan view)
$\Delta N'$	increment in yawing moment about ζ' axis due to effect of edge suction force when moment center is aft of the leading edge
C_n	yawing-moment coefficient $\left(\frac{N}{qSb} \right)$
M	rolling moment about ξ' axis
L	lift
β	sideslip angle (positive when sideslipping to right), degrees
$C_{n\beta}$	yawing-moment-due-to-sideslip stability derivative $\left(\frac{\partial C_n}{\partial \beta} \right)$ measured about ζ axis
$C_{n\beta}'$	yawing-moment-due-to-sideslip stability derivative measured about ζ' axis
$C_{l\beta}'$	rolling-moment-due-to-sideslip stability derivative measured about ξ' axis

M_1	free-stream Mach number
B	$\sqrt{M_1^2 - 1}$
μ	Mach angle (arc tan $\frac{1}{B}$)
m	slope of right wing tip measured from line parallel to plane of symmetry in plane of wing (positive for raked-out tip, negative for raked-in tip)
B_m	ratio of tangent of right tip angle to tangent of Mach cone angle $\left(\frac{m}{\tan \mu} \right)$
$F(\phi, k)$	incomplete elliptic integral of the first kind with modulus k
$E(\phi, k)$	incomplete elliptic integral of the second kind with modulus k
α	angle of attack, radians

The body axes are generally a right-handed system of three orthogonal axes as shown in figure 1 with the longitudinal axis ξ' lying in the plane of the wing. The stability axes are, in effect, the body axes rotated about the lateral axis η' (through $-\alpha$) until the longitudinal axis is in the plane of the free-stream vector; a subsequent rotation about the vertical axis ζ (through β) would bring the longitudinal axis in line with the free-stream vector and the axes would now be coincident with the wind axes.

METHOD OF ANALYSIS

With respect to a system of body axes, there is no component of the normal force in the chordwise direction; and likewise, for a wing in sideslip there is no component of the normal force that will produce a yawing moment about the vertical body axis. On the other hand, the forces produced by the edge suction lie in the plane of the wing and provide the only yawing moment due to sideslip about the ζ' axis of the body-axes system. The system of axes most commonly used in the dynamic stability calculations, however, are the stability axes and it would be most practical to present the

stability derivatives for this system of axes. According to the procedure given in reference 3, the stability axes can be obtained by rotating the body axes through an angle of $-\alpha$ about the η' axis or transverse axis of the airplane, and the expression for the derivative coefficients for the yawing moment due to sideslip is then

$$C_{n\beta} = C_{n\beta}' \cos \alpha - C_{l\beta}' \sin \alpha$$

where $C_{n\beta}'$ and $C_{l\beta}'$ are the derivative coefficients for the yawing and rolling moment in sideslip about the body axes. Since the angle of attack α is necessarily a small quantity to comply with the thin-airfoil-theory calculations used herein, it is sufficient to write

$$C_{n\beta} = C_{n\beta}' - C_{l\beta}' \alpha$$

The $C_{l\beta}'$ term in the expression can be obtained directly from reference 2 for all the plan forms considered and the only additional calculations required, therefore, are the moments due to the edge-suction forces. The calculation of these moments will be based on the assumption that the Kutta-Joukowski condition holds for all subsonic trailing edges. It is possible that this assumption might not be valid for a fairly rounded edge raked at a very small angle from the free-stream direction. In this case it would be necessary to assume or specify some other condition on the trailing edge. But if the analysis were to hold for a finite range of sideslip angles, such as considered herein, it also would be necessary to specify the manner of transition and the angle at which transition from the assumed condition to the Kutta-Joukowski condition takes place. Since there is no method available at present for predicting or specifying such phenomena, it is most practical to impose the Kutta-Joukowski condition for all finite angles of sideslip.

Prediction of the resultant effects of edge suction is somewhat difficult. Theoretically, infinite perturbation velocities normal to a leading edge cause infinite pressures which, when acting on an edge of zero radius, yield a finite suction force. The existence and magnitude of the force have been well verified experimentally in subsonic flow. Actually, the infinite pressure at the leading edge is never fully realized because of viscous effects, but the rounded leading edges compensate for the drop in pressure and the net

resultant suction force is close to the theoretical value. In evaluating the applicability of the estimated suction forces in supersonic flow, however, it must be realized that the trend in airfoil sections is toward thinner and considerably less rounded edges. The edge-suction effect on the edges subjected to subsonic-type flow, therefore, probably will not be as fully realized on supersonic airfoils as it was on the subsonic airfoils. The complete theoretical value will be used in this analysis, however, since no really practical evaluation of the extent to which the suction effect will be realized is available. On the other hand, it would be safe to predict that, as the angle of sweep is increased, the angle-of-attack range over which the edge suction is materially realized will be reduced in a manner corresponding to the reduction in the angle of attack permissible before leading-edge separation and drag rise occur as the angle of sweep is increased. (See reference 7.) If the calculated effects of edge suction were to be completely disregarded, the value of $C_{n\beta}$ due to the normal force distribution on the wing would be merely a times the values for $C_{l\beta}$ given in reference 2.

Of the methods advanced for the calculation of edge-suction forces on wings at supersonic speeds (references 8, 9, and 10), the method employing the perturbation velocity normal to the leading edge was followed in this investigation.

The steps involved in determining the suction force are outlined in references 4 and 8. Since the distribution of the force along the edge was found to be a linear function of the distance from the junction of the edge and the outlying Mach cone, the center of the suction force is located at two-thirds the length of the edge. The yawing moment can be obtained quite simply, therefore, as soon as the plan form and moment center are specified. For the numerical results presented in this report the moment center is considered as located at the origin of the axes, that is, at the leading edge of the root chord. The component of the normal force that produces a yawing moment in the lateral plane of the stability axes system lies parallel to the ξ axis. Thus the yawing moment contributed by $C_{l\beta} a$ is independent of the location of the center of rotation along the ξ axis. The yawing moment contributed by the suction forces, however, is dependent on the chordwise location of the point about which the moments are measured. If the moment center is located aft of the leading edge on the root chord, the net change

in yawing moment for positive angles of sideslip is

$$\Delta N' = \frac{-(T_L - T_R) \xi' c.g.}{\sqrt{1+m^2}}$$

where T_L and T_R are the suction forces on the left and right edges of the wing and $\xi' c.g.$ is the location of the moment center aft of the leading edge of the root chord.

The combining of the edge-suction component of the derivative with the normal force component is slightly complicated by the fact that the edge-suction variation with sideslip is more extensively nonlinear. As an edge is rotated from a direction normal to the free stream to a direction parallel to the stream, it passes through the Mach cone and a suction force is initiated. At first the rise in suction force is quite rapid but eventually the curve begins to level off and as the free-stream direction is reached and passed the suction force drops abruptly to zero, due to the Kutta-Joukowski condition. This abrupt drop shows up as a discontinuity in the variation of C_n with β . In general, whenever the edge-suction component is introduced a trend toward nonlinearity in the variation of C_n with β is introduced. For the rectangular plan forms and for any plan form with streamwise tips, the discontinuity in the variation of C_n with β occurs at zero sideslip. (See inset, figs. 4 and 5.) The slope of the yawing-moment curve could be considered as infinite at this point. In order to obtain a better interpretation of the yawing-moment behavior with sideslip, the slope of the curve as the sideslip angle approached zero was taken for the value of the derivative in the study made of the variation of the derivative with aspect ratio and Mach number. In actuality the yawing moment will probably pass through zero sideslip without a discontinuity, and it is evident that a value for the derivative based on a rational variation of yawing moment over a finite range of sideslip angles is hard to obtain theoretically.

The handling of these nonlinear characteristics of the suction effects and the less prominent nonlinear characteristics of the normal-force component will be done as it was in reference 2. The value of the derivative will again be based on the increment in the value of C_n between 0° and 5° of sideslip. Whenever the variation of C_n with β is found to be nonlinear within the first 5° , a supplementary dotted curve will be shown which will give either the value of the derivative for the extent of the sideslip range that

the curve remains linear or the value of the slope at zero sideslip. Further discussion of the procedure used for establishing the value of the derivative will be found in the section on discussion of results.

In order to simplify the analysis and presentation of the results, the plan forms were divided into sectors bounded by the plan-form edges and the Mach cone traces. In Appendix A, the formulas for the yawing moments of the complete plan forms are expressed in symbols representing the moment contributions of the plan-form sectors, or combinations of these sectors, and the moments contributed by the edge suction. These expressions, which do not readily combine and simplify, are given in Appendixes B and C.

Another condition that made desirable the manner of presentation of the moment expressions for a complete plan form was the change in configuration between the Mach cone and wing edge that a wing in sideslip undergoes in supersonic flow. As the tips change from subsonic to supersonic or vice versa, and as the edges and tips change figuratively from leading to trailing edges by swinging past the free-stream direction the normal-force distribution, the suction force, and the yawing moment change considerably. Consequently, it was necessary to divide the sideslip rotation into a number of phases in order that an expression for the yawing moment could be provided for each configuration encountered in the range of sideslip investigated.

The plan forms are classified with regard to the relative positions of the wing tips and the tip Mach cones when the wing is at zero sideslip. The ratio of the tangent of the right tip angle to the tangent of the Mach cone angle B_m makes a convenient index. The slope of the right tip m is defined as positive when the tip is raked out and negative when the tip is raked in. If B_m is equal to or greater than 1, the tips are supersonic leading edges. If B_m is equal to or less than -1 the tips are supersonic trailing edges. For values of B_m between 1 and -1 the tips are subsonic.

DISCUSSION OF RESULTS

The yawing-moment formulas given in Appendix A and the supplementary expressions given in Appendixes B and C constitute the most general results presented in this report. The need for a qualitative interpretation of these expressions was satisfied by calculations of the yawing moments and yawing-moment derivatives with respect to sideslip for a number of plan forms typical of the group

of plan forms analyzed herein. The results of these calculations are presented in graphical form in figures 4 through 10.

The yawing moment stems from two sources: The normal force caused by the pressures acting on the surface of the plan form and the edge-suction force caused by the infinite induced velocities and pressures acting on the edges of the plan form. Only the plan forms having subsonic leading edges are affected immediately by the edge suction at the start of a sideslip. The other plan forms are not affected until the sideslip angle is great enough to make some edge a subsonic leading edge. Many of the curves, therefore, are made up for the most part of the yawing component due to the normal-force distribution resulting from a sideslip. In effect these curves or portions of these curves were available directly from reference 2 in the form of the rolling moment due to sideslip which is easily converted to the yawing moment about the stability axes.

It might be well also to point out that the sideslip range for the swept-back wings has been somewhat restricted as it was in reference 2. Although the analysis for the swept-back plan forms could have been carried to greater sideslip angles by the methods applied in reference 2 and in this report, the complexity of the calculation warranted the limitation of the sideslip angles to a useful minimum.

Variation of $\frac{C_n}{\alpha^2}$ with β

From inspection of the curves in figures 4 and 5 showing the variation of $\frac{C_n}{\alpha^2}$ with β it is evident that at least for the Mach numbers corresponding to these curves ($B = 1$ and $B = \frac{4}{3}$) there is a small range of linear variation of yawing moment with sideslip angle. The breaks, or discontinuities in the slopes of the curves, occur at phase changes and are due to the normal-force component as well as the edge-suction effects. The jumps, or discontinuities in the curves themselves, are caused by the edge-suction component as an edge passes through the free-stream direction and changes from a trailing edge to a leading edge or vice versa. The other nonlinear trends in the curves are due for the most part to the edge-suction effects.

The only curves in figures 4 and 5 that show directional stability (positive slope) in the first phase of the C_n variation with β are the curves for the subsonic triangular and swept-back

plan forms and the subsonic-edged trapezoidal plan forms with raked-out tips. The other curves, including the rectangular plan-form curve which has the discontinuity at zero sideslip, have negative slopes corresponding to directional instability. As will be shown later, at different Mach numbers and different aspect ratios the slopes of the curves change and in some cases reverse in sign. For a few of the plan forms, notably the supersonic-edged triangular plan form and the trapezoidal plan form with subsonic raked-out tips, the curves undergo a reversal in sign when the second or third phase (Appendices A and B) is reached.

As mentioned in the discussion of the method of analysis, the establishment of a value for the stability derivative $C_{n\beta}$ was handled in the manner adopted in reference 2. The problem therein, as well as herein, was the complexity of the expressions for C_n which made the differentiation with respect to β impractical. The derivatives were finally based on the value of C_n at 5° of sideslip. If the variation of C_n with β was determined to be nonlinear within the first 5° of sideslip, a dotted curve (such as shown in figs. 6 through 10) representing the value of the derivative for whatever range linearity did exist was used to supplement the curve based on the value of C_n at 5° of sideslip. In this way not only is a reasonably accurate value of the stability derivative provided but an indication is given also as to whether the linearity of the C_n variation with β exists out to 5° of sideslip. The direction of the change in trend of the C_n variation with β is indicated also by this use of the solid curve in conjunction with the dotted curve.

Variation of $\frac{C_{n\beta}}{\alpha^2}$ with Aspect Ratio and Mach Number

The results of the calculations made to investigate the variations of the stability derivatives with aspect ratio and Mach number are presented in figures 6 through 10. The discussion of these variations will be divided into two sections: One on the effects of the normal force component and one on the effects of the edge-suction component. Consequently any qualification of the edge-suction results can be accomplished quite readily whenever applicable edge-suction data become available.

Normal force effects.— The normal-force contribution to the yawing moment can be summed up quite readily from the data presented in reference 2. The rectangular plan forms of very low aspect ratio

($A < 1.635$) and the trapezoidal plan forms of moderately low aspect ratio ($A \approx 4$) with raked-out tips provided positive directional stability throughout the Mach number range investigated. At the larger aspect ratios these two plan forms yielded directional instability over at least part of the Mach number range. The triangular plan forms and the swept-back plan forms provided directional stability as long as their leading edges remained subsonic, but the sign of the derivative changed when the leading edge became supersonic. The trapezoidal plan forms with raked-in tips yielded directional instability with subsonic tips but achieved neutral stability over a limited sideslip range when the tips became supersonic. The general trend of the variation of $C_{n\beta}$ with Mach number and aspect ratio was a reduction in the magnitude of the derivative with an increase in these parameters.

Effects of edge suction.— With the inclusion of leading-edge suction effect the subsonic-edged triangular and swept-back wings received considerable increase in directional stability. The supersonic-edged triangular and swept-back plan forms, and the trapezoidal plan forms with supersonic raked-out tips did not experience any suction effect until the second phase was reached. Consequently, the value of the derivative based on the first-phase sideslip angles remained unchanged from the value contributed by the normal force. The trapezoidal plan forms with subsonic raked-out tips received an increase in directional stability with the inclusion of the suction effects. The trapezoidal plan forms with raked-in tips, either subsonic or supersonic, and the inverted triangular plan forms were not affected by leading-edge suction within the sideslip range used to determine the derivative. The effect of edge suction on the derivative for the rectangular wing was a trend toward more positive directional stability although the discontinuity in the curve at zero sideslip resulted in an increase in the magnitude of the unstable yawing moments.

The only remarkable change in the variation of the derivatives with aspect ratio or with Mach number was the increase in the value of the derivative for the subsonic triangles as the leading edges of these plan forms approached the Mach cones (i.e., as B_m approached 1) in the initial position of zero sideslip.

These evaluations of the effects of edge suction can be considered typical, but at the same time it must be remembered that they are not completely indicative for all the plan forms within the bounds of the family investigated. The suction effect can be either stabilizing or destabilizing, depending on the relative location of

the edge-suction vector with respect to the moment center. Thus in some cases a small change in the slope of the edge or in the span of the plan forms with raked-in tips, or a chordwise shift in the moment center, might possibly reverse the sign of the moment contributed by the suction effect.

CONCLUDING REMARKS

For most of the plan forms and conditions investigated, the variation of the yawing moment with sideslip was sufficiently linear to establish a value for the derivative that was valid out to 5° of sideslip.

Measuring moments about the vertical axis of a stability-axes system with the origin located at the leading edge of the root chord in all cases, the yawing moment due to sideslip was found to provide directional stability for the subsonic-edged triangular and swept-back plan forms, and for a limited range of raked-out trapezoidal plan forms and rectangular plan forms. In general, only raked-out trapezoidal and rectangular plan forms of rather low aspect ratio ($A \approx 4$ and $A \approx 2$, respectively) were found to be directionally stable throughout the Mach number range ($M_1 = 0$ to $M_1 = 4.9$) considered. The other plan forms investigated, supersonic-edged triangular and swept-back plan forms and trapezoidal plan forms with raked-in tips, were directionally unstable or neutrally stable.

Adding the edge-suction contributions to the normal-force yawing moments had its greatest effect in increasing the magnitude of the already stable derivatives. The edge suction did not, in general, affect the unstable derivatives, since they were associated mainly with supersonic-edged plan forms. A conspicuous nonlinear effect was incurred by the edge-suction forces as an edge of a plan form passed through the free-stream direction. The sudden appearance or disappearance of the suction force at this time caused a sudden jump in the yawing moment. This discontinuity in the yawing-moment variation with sideslip occurs at zero sideslip for the rectangular plan form and tends to invalidate the values of the derivative calculated for this plan form.

Ames Aeronautical Laboratory,
National Advisory Committee for Aeronautics,
Moffett Field, Calif.

APPENDIX A

FORMULAS FOR YAWING MOMENT DUE TO SIDESLIP
General Restriction: $\tan \beta \leq B$

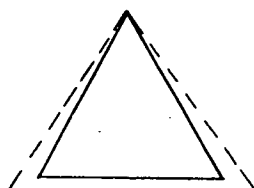
TRIANGULAR WINGS

Subsonic Tips

$Bm < 1$

$C_n = \frac{N}{qSb} = \frac{N}{2qc_r s_m^2}$

$m \geq \frac{1}{B + \sqrt{B^2 + 1}}^a$



Phase 1, $0 \leq \tan \beta \leq \left(\frac{1-Bm}{B+m} \right)$

$N = N'_A - \alpha M_A$



Phase 2, $\left(\frac{1-Bm}{B+m} \right) \leq \tan \beta \leq m$

$N = N'_C - \alpha M_C$



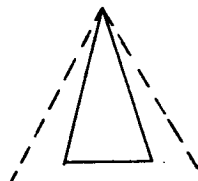
Phase 3, $m \leq \tan \beta \leq \left(\frac{1+Bm}{B-m} \right)$

$N = -\alpha M_D$



^a Right edge crosses Mach cone before left edge crosses x axis.

$$m < \frac{1}{B + \sqrt{B^2 + 1}}$$



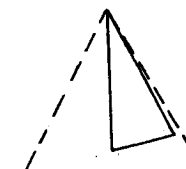
Phase 1, $0 \leq \tan \beta \leq m$

$$N = N'_A - \alpha M_A$$



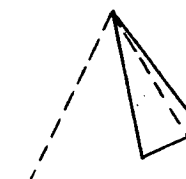
Phase 2, $m \leq \tan \beta \leq \left(\frac{1-Bm}{B+m} \right)$

$$N = N'_B - \alpha M_B$$



Phase 3, $\left(\frac{1-Bm}{B+m} \right) \leq \tan \beta \leq \left(\frac{1+Bm}{B-m} \right)$

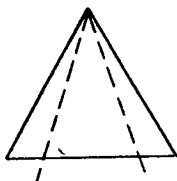
$$N = - \alpha M_D$$



Supersonic Tips

$$Bm \geq 1$$

$$C_n = \frac{N}{qSb} = \frac{N}{2qc_r^3 m^2}$$



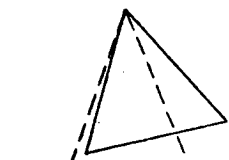
Phase 1, $0 \leq \tan \beta \leq \left(\frac{Bm-1}{B+m} \right)$

$$N = - \alpha M_E$$

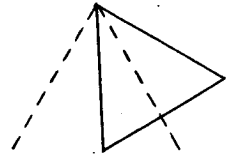


Phase 2, $\left(\frac{Bm-1}{B+m} \right) \leq \tan \beta \leq m$

$$N = N'_C - \alpha M_C$$

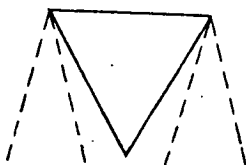


Phase 3, $m \leq \tan \beta \leq \left(\frac{1+Bm}{B-m} \right)$



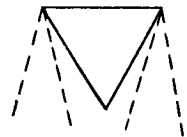
$$N = - \alpha M_D$$

$$Bm \leq -1$$



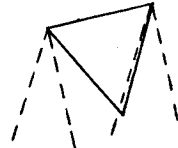
$$C_n = \frac{N}{qSb} = \frac{N}{2qc_r s_m^2}$$

Phase 1, $0 \leq \tan \beta \leq -\left(\frac{Bm+1}{B-m} \right)$



$$N = 0$$

Phase 2, $-\left(\frac{Bm+1}{B-m} \right) \leq \tan \beta \leq -m$



$$N = - \alpha M_F$$

Phase 3, $-m \leq \tan \beta \leq \left(\frac{1-Bm}{B+m} \right)$

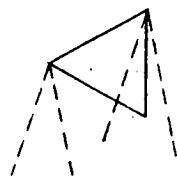
$$N = N' G - \alpha M_G$$

SWEPT-BACK WINGS

Subsonic Tips

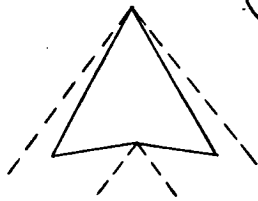
$$Bm < 1$$

$$C_n = \frac{N}{qSb} = \frac{N}{q(b^2 c_r / 2)}$$



$$m \geq \frac{1}{B + \sqrt{B^2 + 1}}$$

$$0 \leq (l - c_r) \leq \frac{l(B^2 + 2Bm - 1)}{\left(-B^2 + 2\frac{B}{m} + 1\right)}$$



$$\text{Phase 1, } 0 \leq \tan \beta \leq \frac{1 - Bm}{B + m}$$

$$N = N_A' - \alpha(M_A - M_H)$$

$$\frac{l(B^2 + 2Bm - 1)^b}{\left(-B^2 + 2\frac{B}{m} + 1\right)} \leq (l - c_r) \leq Bml^c$$

$$\text{Phase 1, } 0 \leq \tan \beta \leq \frac{Bml - (l - c_r)}{B(l - c_r) + lm}$$



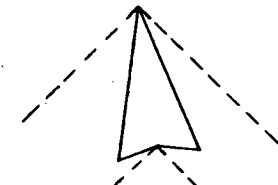
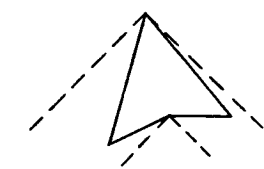
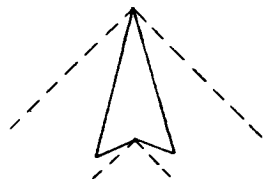
$$N = N_A' - \alpha(M_A - M_H)$$

$$m < \frac{1}{B + \sqrt{B^2 + 1}}$$

$$0 \leq (l - c_r) \leq \frac{l(B^2 + 2Bm - 1)}{\left(-B^2 + 2\frac{B}{m} + 1\right)}$$

$$\text{Phase 1, } 0 \leq \tan \beta \leq m$$

$$N = N_A' - \alpha(M_A - M_H)$$

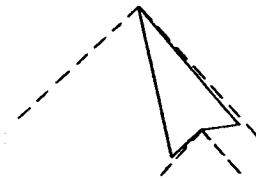


^b Inside left edge hits Mach cone from cutout before right leading edge becomes supersonic.

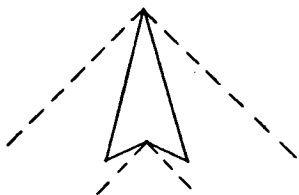
^c Prevents Mach cone at cutout from crossing wing at zero sideslip.

$$\text{Phase 2, } m \leq \tan \beta \leq \frac{1-Bm}{B+m}$$

$$N = N'_{B'} - \alpha(M_B - M_I)$$

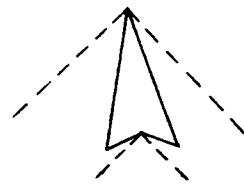


$$\frac{l(B^2+2Bm-1)^d}{(-B^2+2\frac{B}{m}+1)} \leq (l-c) \leq lm \left(\frac{B-m}{Bm+1} \right)^e$$

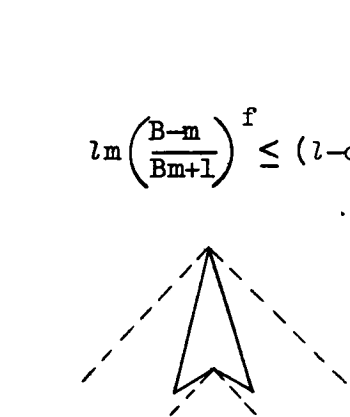


$$\text{Phase 1, } 0 \leq \tan \beta \leq m$$

$$N = N'_{A'} - \alpha(M_A - M_H)$$

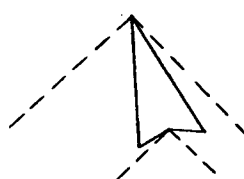


$$\text{Phase 2, } m \leq \tan \beta \leq \frac{Blm - (l-c_r)}{B(l-c_r) + lm}$$



$$\text{Phase 1, } 0 \leq \tan \beta \leq \frac{Blm - (l-c_r)}{B(l-c_r) + lm}$$

$$N = N'_{A'} - \alpha(M_A - M_H)$$



^dInside left edge hits Mach cone from cutout before right leading edge becomes supersonic.

^eLeft leading edge swings past x axis before inside left edge hits Mach cone from cutout.

^fInside left edge hits Mach cone from cutout before left leading edge swings past x axis.

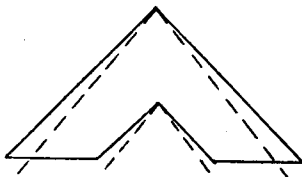
Supersonic Tips

 $B_m \geq 1$

$$C_n = \frac{N}{qSb} = \frac{N}{qbm \left[l \left(\frac{b}{2m} + 2c_r \right) - l^2 - c_r^2 \right]}$$

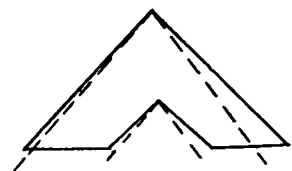
$$m < \frac{2B}{B^2 - 1} \quad g$$

$$0 \leq (l - c_r) \leq \frac{l \left(-B^2 + \frac{2B}{m} + 1 \right)}{(B^2 + 2Bm - 1)}$$

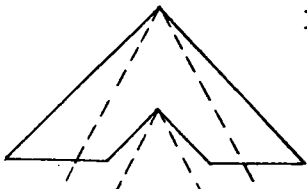


$$\text{Phase 1, } 0 \leq \tan \beta \leq \left(\frac{B_m - 1}{B + m} \right)$$

$$N = -\alpha(M_E - M_J)$$



$$\frac{l \left(-B^2 + \frac{2B}{m} + 1 \right)^h}{(B^2 + 2Bm - 1)} \leq (l - c_r) \leq \frac{l^i}{mB}$$



$$\text{Phase 1, } 0 \leq \tan \beta \leq \frac{l - B_m(l - c_r)}{B_l + m(l - c_r)}$$

$$N = -\alpha(M_E - M_J)$$



^gPrevents ξ axis from crossing Mach cone at right before left edge hits Mach cone.

^hInside right edge hits apex Mach cone before left leading edge hits apex Mach cone.

ⁱPrevents cutout from overlapping apex Mach cone at zero sideslip.

$$\text{Phase 2, } \frac{l-Bm(l-c_r)}{Bl+m(l-c_r)} \leq \tan \beta \leq \frac{Bm-l}{B+m}$$



$$N = -\alpha(M_E - M_K)$$

TRAPEZOIDAL WINGS

Subsonic tips

Span limitation

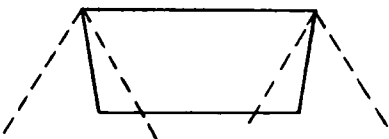
$$0 > Bm > -1$$

$$\tan \beta \leq \frac{B(b+c_r m) - c_r}{Bc_r + b + c_r m}$$

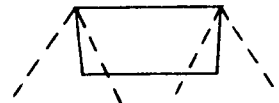
$$C_n = \frac{N}{qSb} = \frac{N}{qc_r b(b+c_r m)}$$

$$-m \leq \frac{1}{B + \sqrt{B^2 + 1}}$$

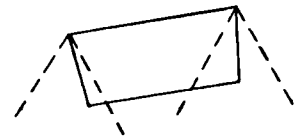
Phase 1, $0 < \tan \beta < -m$



$$N = -\alpha[M_O + M_S + M_N - (L_O - L_N) b/2]$$



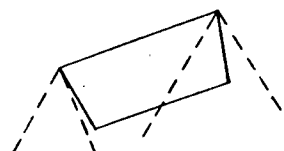
$$\text{Phase 2, } -m \leq \tan \beta \leq \frac{1+Bm}{B-m}$$



$$N = N'_P - \alpha [M_P + M_S + M_N - (L_P - L_N) b/2]$$

$$\text{Phase 3, } \frac{1+Bm}{B-m} \leq \tan \beta \leq \frac{1-Bm}{B+m}$$

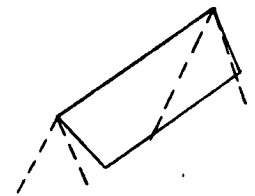
$$N = N'_P - \alpha(M_P + M_T - L_P b/2)$$



Phase 4, $\frac{1-Bm}{B+m} \leq \tan \beta \leq \frac{\text{Span}}{\text{limitation}}$

$$N = -\alpha [M_V + M_Q + M_T - (L_V + L_Q) b/2]$$

$$-m > \frac{1}{B + \sqrt{B^2 + 1}}$$



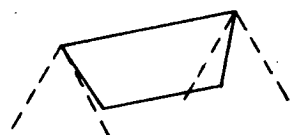
Phase 1, $0 \leq \tan \beta \leq \frac{1+Bm}{B-m}$

$$N = -\alpha [M_O + M_S + M_N - (L_O - L_N) b/2]$$



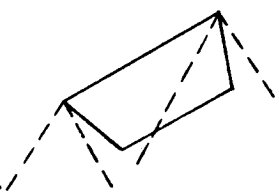
Phase 2, $\frac{1+Bm}{B-m} \leq \tan \beta \leq -m$

$$N = -\alpha (M_O + M_T - L_O b/2)$$



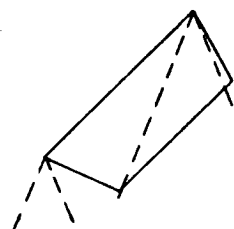
Phase 3, $-m \leq \tan \beta \leq \frac{1-Bm}{B+m}$

$$N = N'_P - \alpha (M_P + M_T - L_P b/2)$$



Phase 4, $\frac{1-Bm}{B+m} \leq \tan \beta \leq \frac{\text{Span}}{\text{limitation}}$

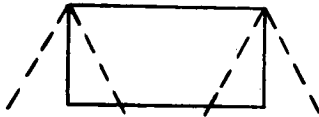
$$N = -\alpha [M_V + M_Q + M_T - (L_V + L_Q) b/2]$$



$B_m = 0$ (Rectangular)

Span limitation

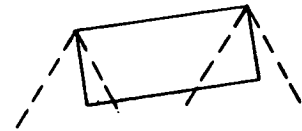
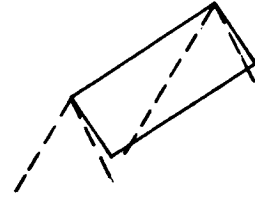
$$\tan \beta \leq \frac{Bb - c_r}{Bc_r + b}$$



$$C_n = \frac{N}{qSb} = \frac{N}{qc_r b^2}$$

Phase 1, $0 \leq \tan \beta \leq 1/B$

$$N = N'_P - \alpha [M_P + M_S + M_N - (L_P - L_N) b/2]$$

Phase 2, $1/B \leq \tan \beta \leq$ Span limitation

$$N = -\alpha [M_V + M_Q + M_T - (L_V + L_Q) b/2]$$

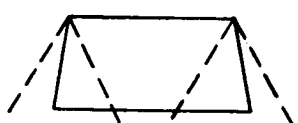
 $0 < B_m < 1$

Span limitation

$$\tan \beta \leq \frac{B(b - mc_r) - c_r}{Bc_r + b - mc_r}$$

$$C_n = \frac{N}{qSb} = \frac{N}{qc_r b(b - mc_r)}$$

$$m \leq \frac{1}{B + \sqrt{B^2 + 1}}$$

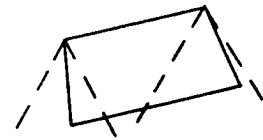
Phase 1, $0 \leq \tan \beta \leq m$

$$N = N'_P + N'_M - \alpha [M_P + M_R + M_M - (L_P - L_M) \left(\frac{b}{2} - mc_r \right)]$$



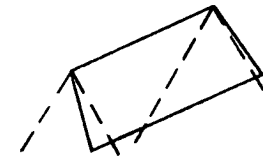
Phase 2, $m \leq \tan \beta \leq \frac{1-Bm}{B+m}$

$$N = N'P - \alpha \left[M_P + M_R + M_N - (L_P - L_N) \left(\frac{b}{2} - mc_r \right) \right]$$



Phase 3, $\frac{1-Bm}{B+m} \leq \tan \beta \leq \frac{1+Bm}{B-m}$

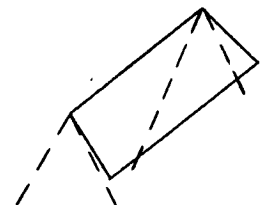
$$N = -\alpha \left[M_V + M_Q + M_R + M_N - (L_V + L_Q - L_N) \left(\frac{b}{2} - mc_r \right) \right]$$



Phase 4, $\frac{1+Bm}{B-m} \leq \tan \beta \leq \frac{\text{Span}}{\text{limitation}}$

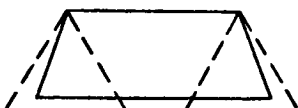
$$N = -\alpha \left[M_V + M_Q + M_T \right]$$

$$- (L_V + L_Q) \left(\frac{b}{2} - mc_r \right)$$

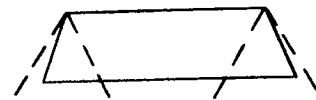


$$m > \frac{1}{B + \sqrt{B^2 + 1}}$$

Phase 1, $0 \leq \tan \beta \leq \frac{1-Bm}{B+m}$

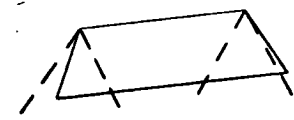


$$N = N'P + N'M - \alpha \left[M_P + M_R + M_M - (L_P - L_M) \left(\frac{b}{2} - mc_r \right) \right]$$



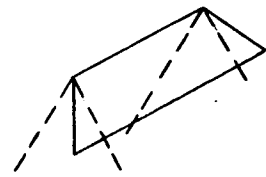
Phase 2, $\frac{1-Bm}{B+m} \leq \tan \beta \leq m$

$$N = N'M - \alpha \left[M_V + M_Q + M_R + M_M - (L_V + L_Q - L_M) \left(\frac{b}{2} - mc_r \right) \right]$$



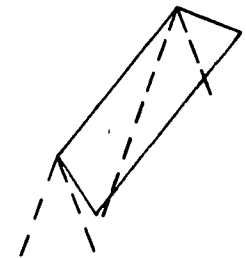
Phase 3, $m \leq \tan \beta \leq \frac{1+Bm}{B-m}$

$$N = -\alpha \left[M_V + M_Q + M_R + M_N - (L_V + L_Q - L_N) \left(\frac{b}{2} - mc_r \right) \right]$$



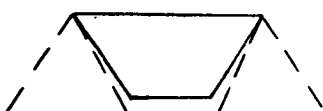
Phase 4, $\frac{1+Bm}{B-m} \leq \tan \beta \leq \frac{\text{Span}}{\text{limitation}}$

$$N = -\alpha \left[M_V + M_Q + M_T - (L_V + L_Q) \left(\frac{b}{2} - mc_r \right) \right]$$



Supersonic Tips

$$Bm \leq -1$$



Span limitation

$$\tan \beta \leq \frac{B(mc_r + b) - c_r}{Bc_r + b + mc_r}$$

$$C_n = \frac{N}{qSb} = \frac{N}{qc_r b(b + mc_r)}$$

Phase 1, $0 \leq \tan \beta \leq -\left(\frac{Bm+1}{B-m}\right)$

$$N = 0$$



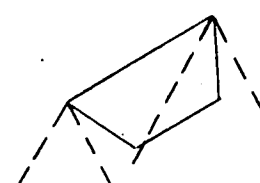
Phase 2, $-\left(\frac{Bm+1}{B-m}\right) \leq \tan \beta \leq -m$

$$N = -\alpha(M_0 + M_T - L_0 b/2)$$



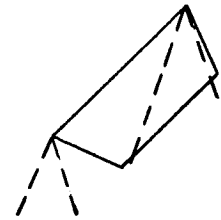
Phase 3, $-m \leq \tan \beta \leq \left(\frac{1-Bm}{B+m}\right)$

$$N = N'_P - \alpha(M_P + M_T - L_P b/2)$$

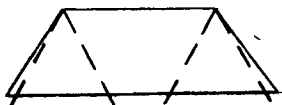


Phase 4, $\left(\frac{1-Bm}{B+m} \right) \leq \tan \beta \leq \frac{\text{Span}}{\text{limitation}}$

$$N = -\alpha [M_V + M_Q + M_T \\ - (L_V + L_Q) b/2]$$



$$Bm \geq 1$$

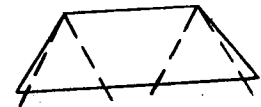


Span limitation
 $\tan \beta \leq \frac{B(b-mc_r) - c_r}{Bc_r + b - mc_r}$

$$C_n = \frac{N}{qSb} = \frac{N}{qc_r b(b-mc_r)}$$

Phase 1, $0 \leq \tan \beta \leq \frac{Bm-1}{B+m}$

$$N = -\alpha [M_V + M_Q + M_R + M_L + M_U \\ - (L_V + L_Q - L_L - L_U) \left(\frac{b}{2} - mc_r \right)]$$



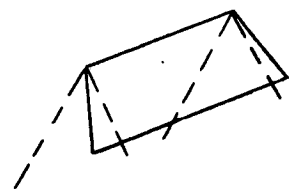
Phase 2, $\frac{Bm-1}{B+m} \leq \tan \beta \leq m$

$$N = N'_M - \alpha [M_V + M_Q + M_R + M_M \\ - (L_V + L_Q - L_M) \left(\frac{b}{2} - mc_r \right)]$$



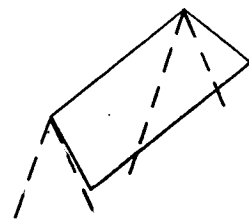
Phase 3, $m \leq \tan \beta \leq \frac{1+Bm}{B-m}$

$$N = -\alpha [M_V + M_Q + M_R + M_N \\ - (L_V + L_Q - L_N) \left(\frac{b}{2} - mc_r \right)]$$



Phase 4, $\frac{1+B_m}{B-m} \leq \tan \beta \leq \frac{\text{Span}}{\text{limitation}}$

$$N = -\alpha \left[M_V + M_Q + M_T - (L_V + L_Q) \left(\frac{b}{2} - mc_r \right) \right]$$

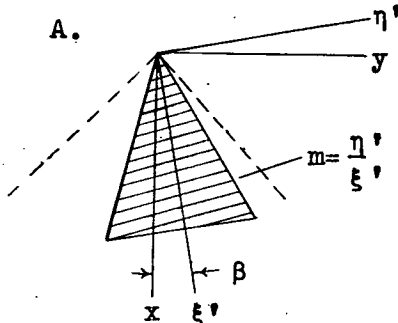


APPENDIX B

SUMMARY OF ROLLING-MOMENT AND ESSENTIAL LIFT EXPRESSIONS
 TO BE USED IN CALCULATION OF YAWING MOMENTS
 CONTRIBUTED BY NORMAL FORCES

Triangular Wings

A.



$$M_A = \frac{-2\pi a q c_r s_m^2 \sin \beta}{3E} \sqrt{\frac{G}{Bm}}$$

where

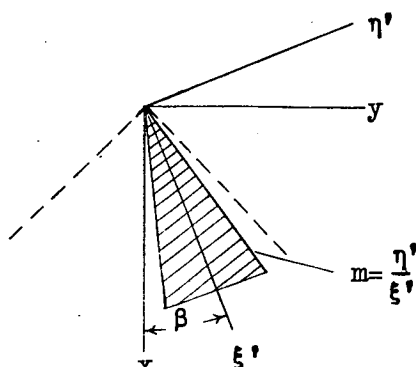
E is the complete elliptic integral of the second kind with modulus

$$\sqrt{1-G^2}$$

$$G = \frac{(1-m^2 \tan^2 \beta) + B^2 (m^2 - \tan^2 \beta)}{2Bm (1 + \tan^2 \beta)}$$

$$- \sqrt{[(1+m \tan \beta)^2 - B^2(m - \tan \beta)^2] [(1-m \tan \beta)^2 - B^2(m + \tan \beta)^2]} \\ 2Bm (1 + \tan^2 \beta)$$

B.



$$M_B = \frac{-2\pi a q c_r s_m^2 P}{3B} \sqrt{\frac{1-m \tan \beta}{1+m \tan \beta}}$$

when $\tan \beta = m$

$$P = \frac{1}{E} \sqrt{\frac{G_1 Bm}{(1-m^2)}}$$

when $\tan \beta = \frac{1-Bm}{B+m}$

$$P = \frac{\sqrt{2} \sqrt{1+m \tan \beta}}{\pi \sqrt{1+m(\tan \beta) + B(m - \tan \beta)}}$$

when $m < \tan \beta < \frac{1-3m}{B+m}$

$$P = \begin{cases} \frac{[B(m + \tan \beta) - G_1(1-m \tan \beta)](1+m \tan \beta)}{[G_1(1+m \tan \beta) + B(m - \tan \beta)](1-m \tan \beta)(1-G_1)^2} & \frac{G_1 + k'}{G_1 + k'} \\ \frac{k'K}{G_1} + E + \frac{k' \sqrt{1-G_1^2}}{\sqrt{G_1^2 - k'^2}} [E F(\varphi, k) - K E(\varphi, k)] & \end{cases}$$

where

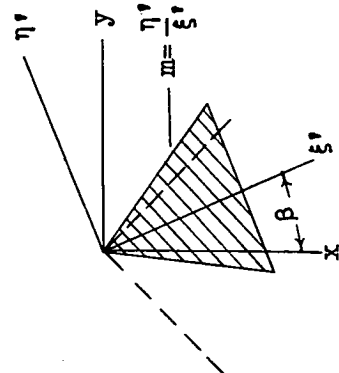
$$G_1 = \frac{(1-m^2 \tan^2 \beta) - B^2(m^2 - \tan^2 \beta) - \sqrt{[(1+m \tan \beta)^2 - B^2(m - \tan \beta)^2] [(1-m \tan \beta)^2 - B^2(m + \tan \beta)^2]}}{2 B \tan \beta (1+m^2)}$$

$$k = \sqrt{1-k'^2} \quad k' = \frac{G_1(1+m \tan \beta) + B(m - \tan \beta)}{(1+m \tan \beta) + G_1 B(m - \tan \beta)}$$

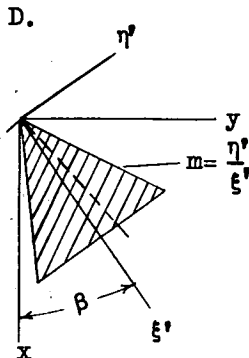
$$\varphi = \arcsin \frac{\sqrt{G_1^2 - k'^2}}{G_1 k}$$

$$K = F\left(\frac{\pi}{2}, k\right)$$

C.

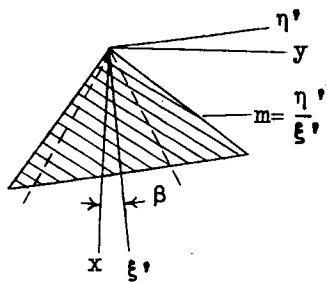


$$M_C = \frac{q a c r^3 \sqrt{2m} [2m^2(B + \tan \beta) - 2m(1+B \tan \beta) - 4m \tan^2 \beta]}{3(B + \tan \beta)^{3/2} \sqrt{m(B - \tan \beta) + (1+B \tan \beta)}}$$



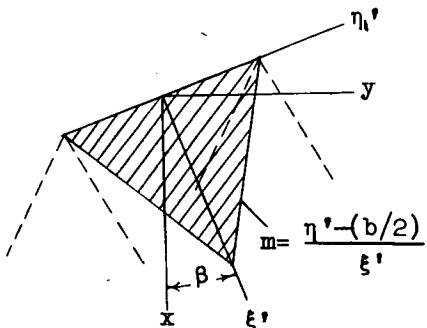
$$M_D = \frac{-q a c_r^3 \sqrt{2m} (m + \tan \beta) [m(B + \tan \beta) + (1 - B \tan \beta)]}{3(B + \tan \beta) \sqrt{m(B - \tan \beta) + (1 + B \tan \beta)}}$$

E.



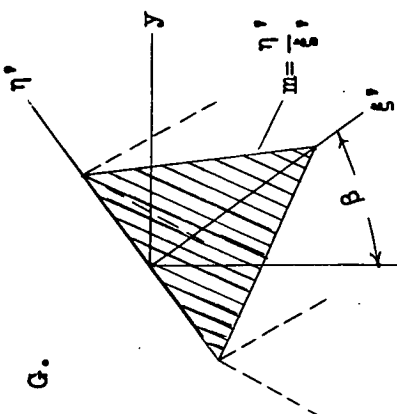
$$M_E = \frac{4q a c_r^3 m (\tan \beta) (1 + \tan^2 \beta)}{3(B^2 - \tan^2 \beta)^{3/2}}$$

F.

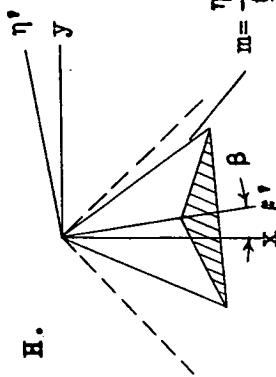


$$M_F = \frac{-\alpha q b^3 m [1 + B(\tan \beta) + m(B - \tan \beta)]}{6 \sqrt{2} \sqrt{B + \tan \beta} [m^2(B - \tan \beta) - m(1 + B \tan \beta)]^{3/2}}$$

$$M_G = \frac{-\alpha q b^3 [11m^2(B - \tan \beta) - 11(B \tan \beta)(1+B \tan \beta) - 2m(1 + \tan^2 \beta)]}{12 \sqrt{2} \sqrt{B + \tan \beta} [m^2(B - \tan \beta) - m(1+B \tan \beta)]^{3/2}}$$



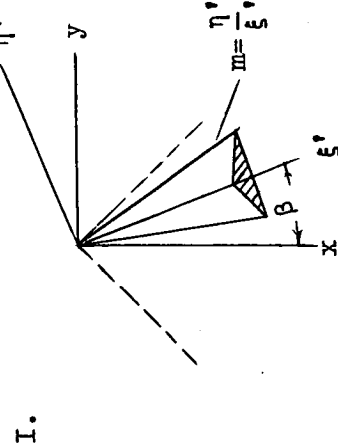
G. Swept-Back Wing Components



$$M_H = \frac{-4\alpha l^3 m^2 \sin \beta}{3E} \sqrt{\frac{G}{Bm}} \left\{ \frac{\pi}{2} - c_r s \left[\frac{3(l-c_r)}{[l^2 - (l-c_r)^2]^2} \right. \right. \\ \left. \left. + \left(\text{arc sin} \frac{l-c_r}{l} + \frac{\pi}{2} \right) \frac{[l^2 + 2(l-c_r)^2]}{[l^2 - (l-c_r)^2]^{5/2}} \right] \right\}$$

where E is the complete elliptic integral of the second kind with modulus $\sqrt{1-G^2}$

$$G = \frac{(1-m^2 \tan^2 \beta) + B^2(m^2 - \tan^2 \beta) - \sqrt{[(1+m \tan \beta)^2 - B^2(m \tan \beta)^2] [(1-m \tan \beta)^2 - B^2(m \tan \beta)^2]}}{2Bm (1 + \tan^2 \beta)}$$

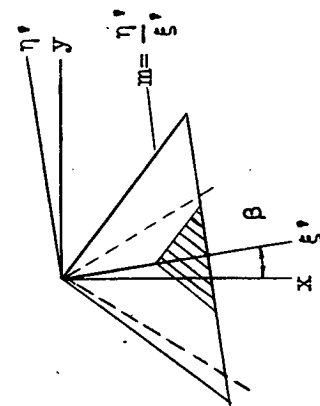


$$M_I = -\frac{4\alpha}{3B} q l^3 m^2 P \sqrt{\frac{1-m}{1+m}} \tan \beta \left(\frac{\pi}{2} - c_r^3 \left\{ \frac{3(l-c_r)}{[l^2 - (l-c_r)^2]^2} \right. \right. \\ \left. \left. + \left[\arcsin \frac{(l-c_r)}{l} + \frac{\pi}{2} \right] \frac{[l^2 + 2(l-c_r)^2]}{[l^2 - (l-c_r)^2]^2} \right\} \right)$$

where P is a factor defined under M_B

J.

$$m > \left(\frac{1+B \tan \beta}{B - \tan \beta} \right)$$



$$M_{J_1} = + \frac{4\alpha q}{3\pi} \left[\sin^{-1} l \left[(1-m \tan \beta) - B^2 (\tan \beta) (m + \tan \beta) \right] + m (l-c_r) \left[(\tan \beta) (1-m) \tan \beta + B^2 (m + \tan \beta) \right] \right. \\ \left. m B (1 + \tan^2 \beta) (2l - c_r) \right]$$

$$\begin{aligned}
& \left\{ \frac{(m + \tan \beta)}{\sqrt{B^2(m + \tan \beta)^2 - (1-m \tan \beta)^2}} \right\} \left\{ -\frac{3m^2 l c_r (l - c_r)}{2} - \frac{3c_r^3 m^2}{8} \right\} \\
& + \sin^{-1} \frac{(1-m \tan \beta) - B^2 (\tan \beta) (m + \tan \beta)}{m B (1 + \tan^2 \beta)} \left\{ \frac{-c_r^3 m^3}{\sqrt{B^2(m + \tan \beta)^2 - (1-m \tan \beta)^2}} \right\} \\
& \left\{ (m + \tan \beta) \left(-\frac{3}{8m} + \frac{(\tan \beta)(1-m \tan \beta) + B^2(m + \tan \beta)}{B^2(m + \tan \beta)^2 - (1-m \tan \beta)^2} \right) \right. \\
& \left. - \frac{3m[(\tan \beta)(1-m \tan \beta) + B^2(m + \tan \beta)]^2}{4[B^2(m + \tan \beta)^2 - (1-m \tan \beta)^2]^2} \right\} \\
& + \frac{m(B^2 - \tan^2 \beta)}{4[B^2(m + \tan \beta)^2 - (1-m \tan \beta)^2]} \left\{ (m - \tan \beta) \left(-\frac{3}{8m} + \frac{(\tan \beta)(1-m \tan \beta) + B^2(m + \tan \beta)}{4[B^2(m + \tan \beta)^2 - (1-m \tan \beta)^2]} \right) \right\} \\
& + \sqrt{(1-B^2 \tan^2 \beta) l^2 + 2(\tan \beta)(B^2 + 1)m l (l - c_r) - (B^2 - \tan^2 \beta)m^2(l - c_r)^2}
\end{aligned}$$

$$\begin{aligned}
& \left\{ (m + \tan \beta) \left(\frac{l^2}{2(B^2 - \tan^2 \beta)} - \frac{c_r^2 m^2}{4[B^2(m - \tan \beta)^2 - (1+m \tan \beta)^2]} \right) \right. \\
& + (m - \tan \beta) \left(\frac{l^2}{2(B^2 - \tan^2 \beta)} - \frac{c_r^2 m^2}{4[B^2(m - \tan \beta)^2 - (1+m \tan \beta)^2]} + \frac{l c_r m^2}{4[B^2(m - \tan \beta)^2 - (1+m \tan \beta)^2]} \right) \\
& - \frac{3c_r^2 m^3 \{ (m + \tan \beta)(1+m \tan \beta) - B^2(m - \tan \beta) \}}{4[B^2(m - \tan \beta)^2 - (1+m \tan \beta)^2]^2} \Big\} \\
& + \sqrt{1 - B^2 \tan^2 \beta} \left\{ -c_r^2 m^3 \right\} \left\{ (m + \tan \beta) \left(\frac{3}{4m[B^2(m + \tan \beta)^2 - (1-m \tan \beta)^2]} \right. \right. \\
& \left. \left. - \frac{3 \{ (m + \tan \beta)(1-m \tan \beta) + B^2(m + \tan \beta) \}}{4[B^2(m + \tan \beta)^2 - (1-m \tan \beta)^2]^2} \right) - \frac{1}{4m[B^2(m - \tan \beta)^2 - (1+m \tan \beta)^2]} \right) \\
& + (m - \tan \beta) \left(\frac{1}{4m[B^2(m + \tan \beta)^2 - (1-m \tan \beta)^2]} - \frac{3}{4m[B^2(m - \tan \beta)^2 - (1+m \tan \beta)^2]} \right)
\end{aligned}$$

$$\begin{aligned}
 & - \frac{3[(\tan \beta)(1+m \tan \beta) - B^2(m - \tan \beta)]}{4[B^2(m - \tan \beta)^2 - (1+m \tan \beta)^2]} \Bigg) \Bigg\} \\
 & + \sin^{-1} \frac{l[(1+m \tan \beta) + B^2(\tan \beta(m - \tan \beta)] + m(l - c_r)[(\tan \beta)(1+m \tan \beta) - B^2(m - \tan \beta)]}{mB(1 + \tan^2 \beta)c_r} \\
 & + \frac{(m + \tan \beta)}{\sqrt{B^2(m - \tan \beta)^2 - (1+m \tan \beta)^2}} \left(\frac{3c_r s_m^2}{8} + \frac{c_r s_m^3[(\tan \beta)(1+m \tan \beta) - B^2(m - \tan \beta)]}{4[B^2(m - \tan \beta)^2 - (1+m \tan \beta)^2]} \right) \\
 & + \frac{(m - \tan \beta)}{\sqrt{B^2(m - \tan \beta)^2 - (1+m \tan \beta)^2}} \left(-\frac{3l c_r s_m^2(l - c_r)}{2} - \frac{c_r s_m^4(B^2 - \tan^2 \beta)}{4[B^2(m - \tan \beta)^2 - (1+m \tan \beta)^2]} \right) \\
 & + \frac{c_r s_m^3[(\tan \beta)(1+m \tan \beta) - B^2(m - \tan \beta)]}{B^2(m - \tan \beta)^2 - (1+m \tan \beta)^2} + \frac{3c_r s_m^4[(\tan \beta)(1+m \tan \beta) - B^2(m - \tan \beta)]^2}{4[B^2(m - \tan \beta)^2 - (1+m \tan \beta)^2]^2} \Bigg\}
 \end{aligned}$$

$$+ \sin^{-1} \frac{(1+m \tan \beta) + B^2 (\tan \beta)(m - \tan \beta)}{m B (1 + \tan^2 \beta)} \left\{ \frac{(m + \tan \beta)}{\sqrt{B^2(m - \tan \beta)^2 - (1+m \tan \beta)^2}} \left(- \frac{3c_r^3 m^2}{8} \right. \right.$$

$$- \frac{c_r^3 m^3 [(\tan \beta)(1+m \tan \beta) - B^2(m - \tan \beta)]}{4[B^2(m - \tan \beta)^2 - (1+m \tan \beta)^2]} + \frac{(m - \tan \beta)}{\sqrt{B^2(m - \tan \beta)^2 - (1+m \tan \beta)^2}} \left(- \frac{3c_r^3 m^2}{8} \right. \right.$$

$$- \frac{c_r^3 m^3 [(\tan \beta)(1+m \tan \beta) - B^2(m - \tan \beta)]}{B^2(m - \tan \beta)^2 - (1+m \tan \beta)^2} - \frac{3c_r^3 m^4 [(\tan \beta)(1+m \tan \beta) - B^2(m - \tan \beta)]^2}{4[B^2(m - \tan \beta)^2 - (1+m \tan \beta)^2]^2}$$

$$+ \frac{c_r^3 m^4 (B^2 - \tan^2 \beta)}{4[B^2(m - \tan \beta)^2 - (1+m \tan \beta)^2]} \left) \right\}$$

$$+ \sin^{-1} \frac{(\tan \beta)(B^2 + 1) l - (B^2 - \tan^2 \beta)m(l - c_r)}{B l (1 + \tan^2 \beta)} \left\{ \frac{l^3 m (\tan \beta)(1 + \tan^2 \beta)}{(B^2 - \tan^2 \beta)^{3/2}} \right\} \left] \right.$$

$$M_{J_2} = + \frac{4\alpha q}{3\pi} \left[- \sin^{-1} \frac{l(\tan \beta(B^2 + 1) + m(l - c_r)(B^2 - \tan^2 \beta))}{Bl(1 + \tan^2 \beta)} \left\{ \frac{l^3 m (\tan \beta(1 + \tan^2 \beta))}{(B^2 - \tan^2 \beta)^{3/2}} \right\} \right]$$

$$- \sin^{-1} \frac{[(1 - m \tan \beta) - B^2(\tan \beta(m + \tan \beta))]l - [(\tan \beta(1 - m \tan \beta) + B^2(m + \tan \beta))m(l - c_r)]}{mB(1 + \tan^2 \beta) c_r}$$

$$\left\{ \frac{m + \tan \beta}{B^2(m + \tan \beta)^2 - (1 - m \tan \beta)^2} \left(\frac{-3l c_r m^2 (l - c_r)}{2} - \frac{c_r^3 m^3 [(\tan \beta(1 - m \tan \beta) + B^2(m + \tan \beta))]}{B^2(m + \tan \beta)^2 - (1 - m \tan \beta)^2} \right) \right.$$

$$+ \frac{3c_r^3 m^4 [(\tan \beta(1 - m \tan \beta) + B^2(m + \tan \beta))]^2}{4[B^2(m + \tan \beta)^2 - (1 - m \tan \beta)^2]} - \frac{c_r^3 m^4 (B^2 - \tan^2 \beta)}{4[B^2(m + \tan \beta)^2 - (1 - m \tan \beta)^2]}$$

$$\left. - \frac{(m - \tan \beta)}{B^2(m + \tan \beta)^2 - (1 - m \tan \beta)^2} \left(\frac{c_r^3 m^3 [(\tan \beta(1 - m \tan \beta) + B^2(m + \tan \beta))]}{4[B^2(m + \tan \beta)^2 - (1 - m \tan \beta)^2]} - \frac{3c_r^3 m^2}{8} \right) \right\}$$

$$\begin{aligned}
 & - \sqrt{(1-B^2 \tan^2 \beta) l^2 - 2(\tan \beta)(B^2 + 1)m l (l - c_r) - (B^2 - \tan^2 \beta)m^2(l - c_r)^2} \\
 & \quad \left\{ (m + \tan \beta) \left(\frac{l^2}{2(B^2 - \tan^2 \beta)} - \frac{c_r^2 m^2}{[B^2(m + \tan \beta)^2 - (1 - m \tan \beta)^2]} \right) \right. \\
 & \quad + \frac{l c_r m^2}{4[B^2(m + \tan \beta)^2 - (1 - m \tan \beta)^2]} + \frac{3c_r^2 m^3 [\tan \beta (1 - m \tan \beta) + B^2(m + \tan \beta)]}{4[B^2(m + \tan \beta)^2 - (1 - m \tan \beta)^2]} \Big\} \\
 & \quad + (m - \tan \beta) \left(\frac{l^2}{2(B^2 - \tan^2 \beta)} - \frac{c_r^2 m^2}{4[B^2(m + \tan \beta)^2 - (1 - m \tan \beta)^2]} \right) \Big\} \\
 & - \sin^{-1} \frac{[(1 + m \tan \beta) + B^2(\tan \beta)(m - \tan \beta)] l - [(\tan \beta)(1 + m \tan \beta) - B^2(m - \tan \beta)] m(l - c_r)}{m B (1 + \tan^2 \beta) (2l - c_r)} \\
 & \quad \left\{ \frac{(m - \tan \beta)}{\sqrt{B^2(m - \tan \beta)^2 - (1 + m \tan \beta)^2}} \left(-\frac{3l c_r m^2(l - c_r)}{2} - \frac{3c_r^3 m^2}{8} \right) \right\} \Big]
 \end{aligned}$$

$$m = \left(\frac{1+B \tan \beta}{B - \tan \beta} \right)^a$$

$$M_{J_1} = + \frac{4\alpha q}{3\pi} \left[\sin^{-1} \frac{2B(m^2+1)l - [2m(B^2-1)+B(3m^2-1)]c_r}{B(m^2+1)(2l-c_r)} \right]$$

$$\left\{ \frac{m^2+2Bm-1}{2\sqrt{m(1+B^2)(mB-1)(m+B)}} \right\} \left\{ -\frac{3lc_r m^2(l-c_r)}{2} - \frac{3c_r^3 m^2}{8} \right\}$$

$$+ \sqrt{m(B^2+1)[2B(m^2+1)lc_r - m(B^2+2Bm-1)c_r^2]} \left\{ \left(\frac{(m^2+2Bm-1)}{1+B^2} \right) \right.$$

$$\left(\frac{l^2}{2(B^2+2Bm-1)} + \frac{lc_r m}{12B(1+m^2)} + \frac{c_r^2 m^2 (B^2+2Bm-1)}{12B^2(1+m^2)^2} \right)$$

$$- \frac{3c_r^2 m}{8B(1+m^2)} \left) + \frac{1}{B(1+B^2)} \left(\frac{l^2(m+2B-B^2m)}{(B^2+2Bm-1)} + \frac{lm(l-c_r)}{2} \right. \right.$$

$$+ \frac{3l^2(mB-1)(m+B)}{2(B^2+2Bm-1)} - \frac{lc_r m [2B(2m^2+1)+m(B^2-1)]}{3B(m^2+1)}$$

$$+ \frac{2l^2m}{5} \left) + \frac{B^2+2Bm-1}{B^2(1+m^2)(1+B^2)} \left(c_r^2 m^2 - \frac{c_r^2 m^2 [2B(2m^2+1)+m(B^2-1)]}{3B(1+m^2)} \right) \right.$$

^aLeft leading edge hits Mach cone from apex.

$$+ \frac{4l c_r m^2}{15} + \frac{4c_r^2 m^3 (B^2 + 2Bm - 1)}{15B(m^2 + 1)} \Big) \Big\}$$

$$+ \sin^{-1} \frac{c_r m (B^2 + 2Bm - 1) - Bl (m^2 + 1)}{Bl (m^2 + 1)} \left\{ \frac{l^3 m (1+m^2) (Bm-1)}{(B^2 + 2Bm - 1)^{3/2} \sqrt{1+B^2}} \right\}$$

$$+ \sin^{-1} \frac{2m(1-B^2) + B(3-m^2)}{B(1+m^2)} \left\{ \frac{c_r^3 m^2}{2\sqrt{m(1+B^2)(mB-1)(m+B)}} \right\}$$

$$\left\{ (m^2 + 2Bm - 1) \left(\frac{3}{8} - \frac{[2m(B^2 - 1) + B(3m^2 - 1)]}{4(m+B)(mB-1)} \right. \right.$$

$$+ \frac{3[2m(B^2 - 1) + B(3m^2 - 1)]^2}{64(m+B)^2(mB-1)^2} - \frac{m(B^2 + 2Bm - 1)}{16(m+B)(mB-1)} \Big)$$

$$+ \frac{3m(B^2 + 2Bm - 1)}{4B} - \frac{[B(3m^2 - 1) + 2m(B^2 - 1)][2B(2m^2 - 1) + 3m(B^2 - 1)]}{4B(m+B)(mB-1)}$$

$$+ \frac{3[B(3m^2 - 1) + 2m(B^2 - 1)]^2}{16B(m+B)(mB-1)} \Big) \Big\}$$

$$+ \sqrt{m(1+B^2)(m+2B-B^2m)} \left\{ \frac{c_r^3 m}{(m+B)} \right\} \left\{ \frac{(m^2 + 2mB - 1)}{(m+B)(1+B^2)} \right\} \left(- \frac{3(m+B)}{16(mB-1)} \right)$$

$$+ \frac{3[2m(B^2-1)+B(3m^2-1)]}{64(mB-1)^2} - \frac{(m+B)^2}{12B(1+m^2)} - \frac{m(B^2+2Bm-1)(m+B)^2}{12B^2(1+m^2)^2}$$

$$+ \frac{3(m+B)^2}{8B(1+m^2)} \Big) + \frac{1}{B(1+B^2)} \left(- \frac{[2B(2m^2-1)+3m(B^2-1)]}{4(mB-1)} + \frac{m+B}{4} \right)$$

$$+ \frac{3[B(3m^2-1)+2m(B^2-1)]}{16(mB-1)} - \frac{m(B^2+2Bm-1)(m+B)}{B(m^2+1)}$$

$$+ \frac{(m+B)[2B(2m^2+1)+3m(B^2-1)]}{3B(m^2+1)} + \frac{m(B^2+2Bm-1)[2B(2m^2+1)+3m(B^2-1)](m+B)}{3B^2(m^2+1)^2}$$

$$- \frac{2(m+B)}{5} - \frac{4m(B^2+2Bm-1)(m+B)}{15B(m^2+1)} - \frac{4m^2(B^2+2Bm-1)^2(m+B)}{15B^2(m^2+1)^2} \Big) \Big\} \Big]$$

$$M_{J_2} = + \frac{4\alpha q}{3\pi} \left[\sin^{-1} \frac{4l(mB-1)(m+B) - [2m(B^2-1)+B(3m^2-1)]c_r}{B(1+m^2)c_r} \right]$$

$$\left\{ \frac{m^2+2mB-1}{2\sqrt{m(1+B^2)(mB-1)(m+B)}} \right\} \left\{ \frac{3lc_r m^2(l-c_r)}{2} + \left(\frac{c_r^3 m^2}{4(mB-1)(m+B)} \right) \right\}$$

$$\left(2m(B^2-1)+B(3m^2-1) - \frac{3[2m(B^2-1)+B(3m^2-1)]^2}{16(m+B)(mB-1)} + \frac{m(B^2+2mB-1)}{4} \right) \Big\}$$

$$+ \sqrt{m(1+B^2) [-4l^2(mB-1)(m+B) + 2lc_r \{ 2m(B^2-1) + B(3m^2-1) \} - c_r^2 m(B^2+2Bm-1)]}$$

$$\left\{ -\frac{(m^2+2mB-1)}{(m+B)(1+B^2)} \left(\frac{l^2(m+B)}{2(B^2+2Bm-1)} - \frac{c_r^2 m}{4(mB-1)} + \frac{lc_r m}{16(mB-1)} \right. \right.$$

$$\left. \left. + \frac{3c_r^2 m [2m(B^2-1) + B(3m^2-1)]}{64(m+B)(mB-1)^2} \right) + \left(\frac{1}{B(m+B)(1+B^2)} \right) \right.$$

$$\left(-\frac{l^2(m+2B-B^2m)(m+B)}{(B^2+2Bm-1)} + \frac{lm(l-c_r)(m+B)}{2} \right.$$

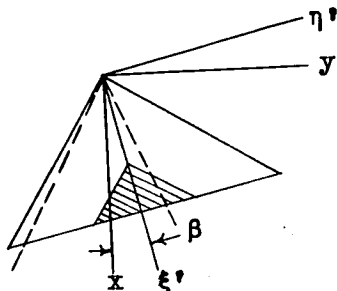
$$\left. - \frac{3l^2(mB-1)(m+B)^2}{2(B^2+2Bm-1)} + \frac{c_r^2 m [2B(2m^2-1) + 3m(B^2-1)]}{4(mB-1)} \right)$$

$$\left. - \frac{lc_r m (m+B)}{4} - \frac{3c_r^2 m [B(3m^2-1) + 2m(B^2-1)]}{16(mB-1)} \right\}$$

$$- \sin^{-1} \frac{l[B(3m^2-1) + 2m(B^2-1)] - c_r m (B^2+2Bm-1)}{Bl(m^2+1)} \left\{ \frac{l^3 m (1+m^2) (mB-1)}{(B^2+2Bm-1)^{3/2} \sqrt{1+B^2}} \right\}$$

$$\begin{aligned}
 & + \sin^{-1} \frac{4l(mB-1)(B+m) - [2m(B^2-1) + B(3m^2-1)]c_r}{B(1+m^2)c_r} \left\{ -\frac{c_r^3 m^2}{8B \sqrt{m(1+B^2)(mB-1)(m+B)}} \right\} \\
 & \left\{ -3m(B^2+2Bm-1) + \frac{[2B(2m^2-1)+3m(B^2-1)][B(3m^2-1)+2m(B^2-1)]}{(m+B)(mB-1)} \right. \\
 & \left. - \frac{3[B(3m^2-1)+2m(B^2-1)]^2}{4(m+B)(mB-1)} \right\}]
 \end{aligned}$$

K.



$$m > \left(\frac{1+B \tan \beta}{B - \tan \beta} \right)$$

$$M_K = M_{J_1} + M_{K_1}$$

$$M_{K_1} = + \frac{2\alpha q}{3} \left[- \frac{l^3 m (\tan \beta)(1 + \tan^2 \beta)}{(B^2 - \tan^2 \beta)^{3/2}} \right]$$

$$+ \frac{(m + \tan \beta)}{\sqrt{B^2(m + \tan \beta)^2 - (1 - m \tan \beta)^2}} \left\{ - \frac{c_r^3 m^3 [(\tan \beta)(1 - m \tan \beta) + B^2(m + \tan \beta)]}{B^2(m + \tan \beta)^2 - (1 - m \tan \beta)^2} \right\}$$

$$- \frac{c_r^3 m^4 (B^2 - \tan^2 \beta)}{4[B^2(m + \tan \beta)^2 - (1 - m \tan \beta)^2]} + \frac{3c_r^3 m^4 [(\tan \beta)(1 - m \tan \beta) + B^2(m + \tan \beta)]^2}{4[B^2(m + \tan \beta)^2 - (1 - m \tan \beta)^2]^2}$$

$$- \frac{3l c_r m^2 (l - c_r)}{2} \}$$

$$+ \frac{(m - \tan \beta)}{\sqrt{B^2(m - \tan \beta)^2 - (1+m \tan \beta)^2}} \left\{ \frac{3c_r^3 m^2}{8} + \frac{3l c_r m^2 (l - c_r)}{2} \right\}$$

$$- \frac{(m - \tan \beta)}{\sqrt{B^2(m + \tan \beta)^2 - (1-m \tan \beta)^2}} \left\{ \frac{c_r^3 m^3 [(m + \tan \beta) + B^2(m + \tan \beta)]}{4[B^2(m + \tan \beta)^2 - (1-m \tan \beta)^2]} \right.$$

$$- \frac{3c_r^3 m^2}{8} \}]$$

$$m = \left(\frac{1+B \tan \beta}{B - \tan \beta} \right)^b$$

$$M_{K_1} = + \frac{2\alpha q}{3} \left[\frac{m^2 + 2Bm - 1}{2\sqrt{m(1+B^2)(mB-1)(m+B)}} \right] \left\{ - \frac{3l c_r m^2 (l - c_r)}{2} \right.$$

$$- \frac{c_r^3 m^2}{4(mB-1)(m+B)} \left(2m(B^2-1) + B(3m^2-1) - \frac{3[2m(B^2-1) + B(3m^2-1)]^2}{16(m+B)(mB-1)} \right)$$

^b Left leading edge hits Mach cone from apex.

$$+ \frac{m(B^2+2mB-1)}{4} \Big) \Big\} - \frac{l^3 m(mB-1)(1+m^2)}{(B^2+2Bm-1)^{3/2} \sqrt{1+B^2}}$$

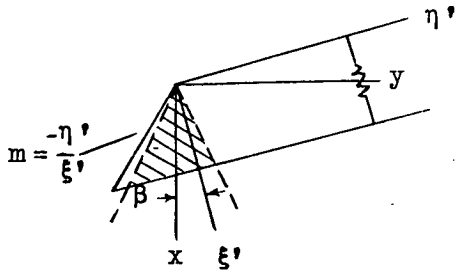
$$- \frac{cr^3 m^2}{8B \sqrt{m(1+B^2)(mB-1)(m+B)}} \left\{ - 3m(B^2+2Bm-1) \right.$$

$$+ \frac{[2B(2m^2-1)+3m(B^2-1)][B(3m^2-1)+2m(B^2-1)]}{(m+B)(mB-1)}$$

$$- \frac{3[B(3m^2-1)+2m(B^2-1)]^2}{4(m+B)(mB-1)} \Big\} \Big]$$

Trapezoidal Wing Components

L.

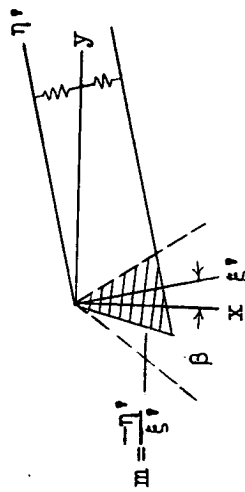


$$L_L = \frac{2q\alpha c_r^2 [B(1 + \tan^2 \beta) + (B^2 - \tan^2 \beta)(m - \tan \beta)]}{(B^2 - \tan^2 \beta)^{3/2}}$$

$$- \frac{2q\alpha c_r^2 (m - \tan \beta)}{\sqrt{B^2 (m - \tan \beta)^2 - (1 + m \tan \beta)^2}} \left[m - \frac{(1 + B \tan \beta)}{(B - \tan \beta)} \right]$$

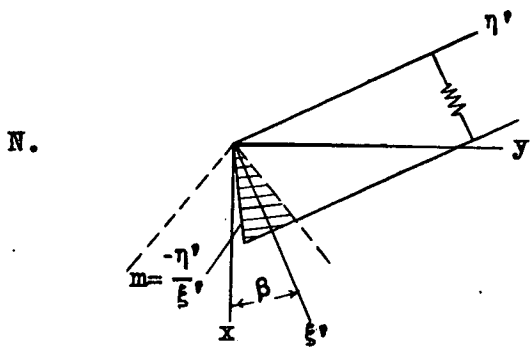
$$M_L = \frac{2q\alpha r^3(m - \tan \beta)}{3\sqrt{B^2 - \tan^2 \beta}} \left\{ \frac{(B^2 + 1) \tan \beta}{(B^2 - \tan^2 \beta)} + m - \frac{B(1 + \tan^2 \beta)[-4(\tan \beta)(B^2 + 1) + B(1 + \tan^2 \beta)]}{2(B^2 - \tan^2 \beta)^2(m - \tan \beta)} \right\}$$

M.



$$M_M = \frac{q\alpha r^2 [3m(B + \tan \beta) + (1 - 3B) \tan \beta - 2 \tan^2 \beta]}{(B + \tan \beta) \sqrt{B^2 - \tan^2 \beta}}$$

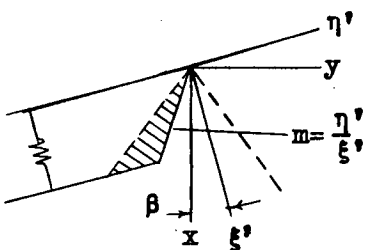
$$M_M = \frac{q\alpha r^3}{12(B + \tan \beta)^2 \sqrt{B^2 - \tan^2 \beta}} \left\{ \frac{4[(B + \tan \beta)(m - \tan \beta)] [3m(B + \tan \beta) - (1 - B \tan \beta)]}{(B + \tan \beta)^2 \sqrt{B^2 - \tan^2 \beta}} \right. \\ \left. + [3m(B + \tan \beta) - 5(1 - B \tan \beta)] [m(B + \tan \beta) + (1 - B \tan \beta)] \right\}$$



$$L_N = \frac{q \alpha c_r^2 [B(m - \tan \beta) + (1+m \tan \beta)]}{(B + \tan \beta) \sqrt{B^2 - \tan^2 \beta}}$$

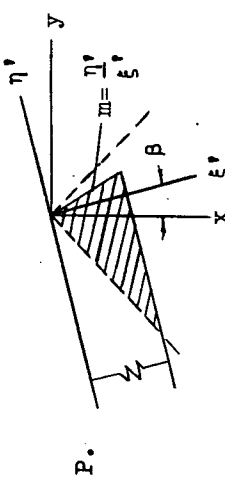
$$M_N = \frac{q \alpha c_r^3 [3m(B + \tan \beta) - 5(1 - B \tan \beta)] [m(B + \tan \beta) + (1 - B \tan \beta)]}{12(B + \tan \beta)^2 \sqrt{B^2 - \tan^2 \beta}}$$

O.



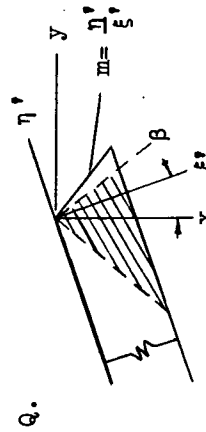
$$L_O = \frac{q \alpha c_r^2 [B(m + \tan \beta) + (1 - m \tan \beta)]}{(B - \tan \beta) \sqrt{B^2 - \tan^2 \beta}}$$

$$M_O = \frac{-q \alpha c_r^3 [3m(B - \tan \beta) - 5(1 + B \tan \beta)] [m(B - \tan \beta) + (1 + B \tan \beta)]}{12(B - \tan \beta)^2 \sqrt{B^2 - \tan^2 \beta}}$$



$$I_P = \frac{qac_r^2 [3m(B - \tan \beta) + (1+3 B \tan \beta - 2 \tan^2 \beta)]}{(B - \tan \beta) \sqrt{B^2 - \tan^2 \beta}}$$

$$M_p = \frac{-q\alpha c_r^3}{12(B - \tan \beta)^2 \sqrt{B^2 - \tan^2 \beta}} \left\{ 4 \left[(B - \tan \beta)(m + \tan \beta) \right] \left[3m(B - \tan \beta) - (1 + B \tan \beta) \right] + \left[3m(B - \tan \beta) - 5(1 + B \tan \beta) \right] \left[m(B - \tan \beta) + (1 + B \tan \beta) \right] \right\}$$

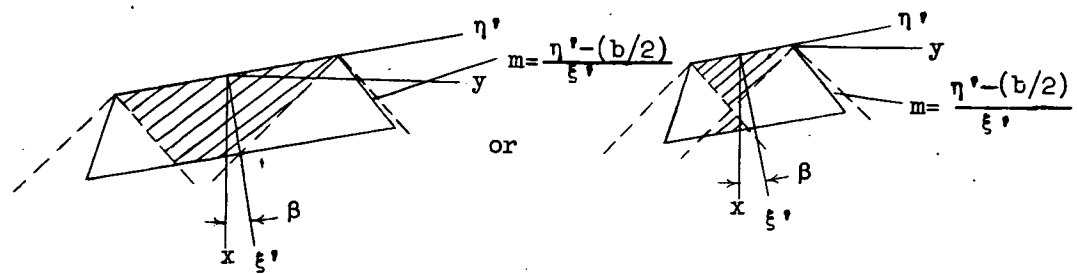


$$I_Q = \frac{2q\alpha\sigma_r^2[B(1+\tan^2\beta)+(B^2-\tan^2\beta)(m+\tan\beta)]}{(B^2-\tan^2\beta)^{3/2}} - \frac{2q\alpha\sigma_r^2(m+\tan\beta)}{\sqrt{B^2(m+\tan\beta)^2-(1-m\tan\beta)^2}} - \left\{ \left[\frac{B(\tan\beta)-1}{B+\tan\beta} \right] + m \right\}$$

$$M_Q = \frac{2gac_x^3(m + \tan \beta)}{3\sqrt{\beta^2 - \tan^2 \beta}} \left\{ \frac{(\beta^2 + 1)}{(\beta^2 - \tan^2 \beta)} \tan \beta - m \right\}$$

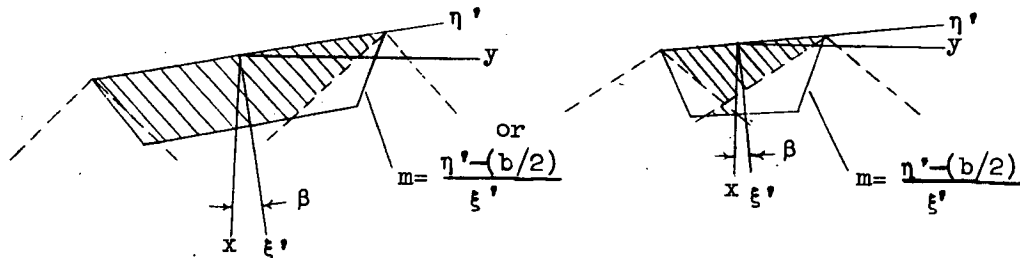
$$+ \frac{B(1+\tan^2 \beta)[4(\tan \beta)(B^2+1)+B(1+\tan^2 \beta)]}{2(B^2-\tan^2 \beta)^2(m+\tan \beta)} \}$$

R.



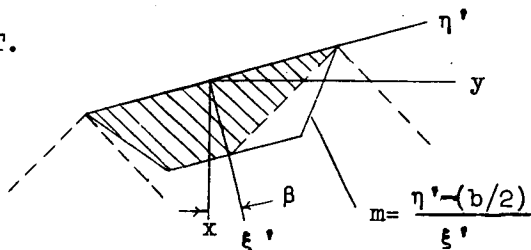
$$M_R = \frac{4\alpha q c_r^2 (1+B^2) \tan \beta}{(B^2 - \tan^2 \beta)^{3/2}} \left[\frac{(b-2c_r m)}{2} - \frac{2c_r B (1 + \tan^2 \beta)}{3(B^2 - \tan^2 \beta)} \right]$$

S.



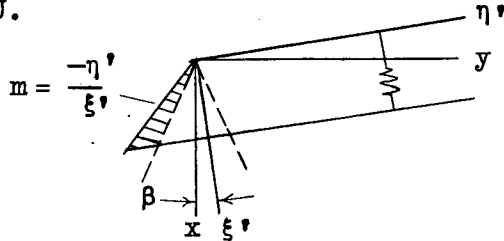
$$M_S = \frac{4\alpha q c_r^2 (1+B^2) \tan \beta}{(B^2 - \tan^2 \beta)^{3/2}} \left[\frac{b}{2} - \frac{2c_r B (1 + \tan^2 \beta)}{3(B^2 - \tan^2 \beta)} \right]$$

T.



$$M_T = \frac{2\alpha q c_r^2}{\sqrt{B^2 - \tan^2 \beta}} \left[\frac{c_r}{3} \left\{ m^2 - \left(\frac{1+B \tan \beta}{B - \tan \beta} \right)^2 \right\} + \frac{b}{2} \left\{ \left(\frac{1+B \tan \beta}{B - \tan \beta} \right) + m \right\} \right]$$

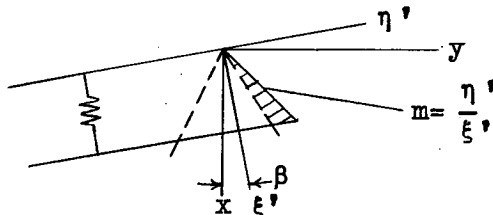
U.



$$L_U = \frac{2\alpha c_r^2 (m - \tan \beta)}{\sqrt{B^2(m - \tan \beta)^2 - (1+m \tan \beta)^2}} \left[m - \frac{(1+B \tan \beta)}{(B - \tan \beta)} \right]$$

$$M_U = \frac{2\alpha c_r^3 (m - \tan \beta)}{3 \sqrt{B^2(m - \tan \beta)^2 - (1+m \tan \beta)^2}} \left[m^2 - \left(\frac{1+B \tan \beta}{B - \tan \beta} \right)^2 \right]$$

V.



$$L_V = \frac{2\alpha c_r^2 (m + \tan \beta)}{\sqrt{B^2(m + \tan \beta)^2 - (1-m \tan \beta)^2}} \left[\left(\frac{B(\tan \beta) - 1}{B + \tan \beta} \right) + m \right]$$

$$M_V = \frac{2\alpha c_r^3 (m + \tan \beta)}{3 \sqrt{B^2(m + \tan \beta)^2 - (1-m \tan \beta)^2}} \left[\left(\frac{B(\tan \beta) - 1}{B + \tan \beta} \right)^2 - m^2 \right]$$

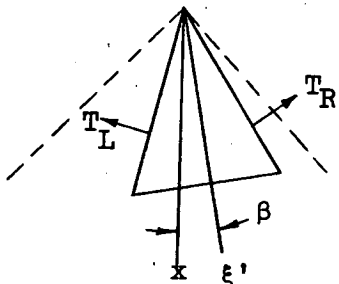
APPENDIX C

SUMMARY OF YAWING MOMENTS DUE TO
SUCTION FORCES

Moments tending to turn plan forms in clockwise rotation are positive and all suction-force vectors shown are located at $2/3$ of the length of the edge measured from its most forward junction with another edge.

TRIANGULAR WINGS

A.



$$N''_A = (T_L - T_R) a - (T_L - T_R) \frac{\xi' c.g.}{\sqrt{1+m^2}}$$

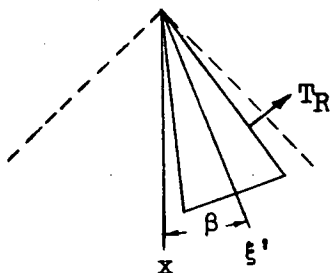
where

$$T_L - T_R = \frac{\pi q \alpha^2 c_r^2 G \sqrt{1+m^2}}{2BE^2 \sqrt{1+\tan^2 \beta}} \left(\sqrt{(1+m^2)(1+\tan^2 \beta) - (B^2+1)(m-\tan \beta)^2} - \sqrt{(1+m^2)(1+\tan^2 \beta) - (B^2+1)(m+\tan \beta)^2} \right)$$

$$a = \frac{2c_r}{3} \sqrt{1+m^2}$$

and G and E are defined under plan form A of Appendix B.

B.



$$N'_B = -T_R a + T_R \frac{\xi' c.g.}{\sqrt{1+m^2}}$$

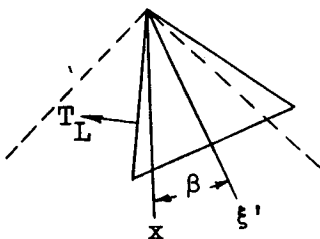
where

$$a = \frac{2c_r \sqrt{1+m^2}}{3}$$

$$T_R = \frac{2\pi q a^2 c_r^2 P^2 m \sqrt{1+m^2} \sqrt{1+\tan^2 \beta} (1-m \tan \beta) \sqrt{(1+m^2)(1+\tan^2 \beta) - (B^2+1)(m+\tan \beta)^2}}{B^3 (m+\tan \beta)^2 (1+m \tan \beta)}$$

and P is defined under plan form B of Appendix B.

C.



$$N'_C = T_L a - T_L \frac{\xi' c.g.}{\sqrt{1+m^2}}$$

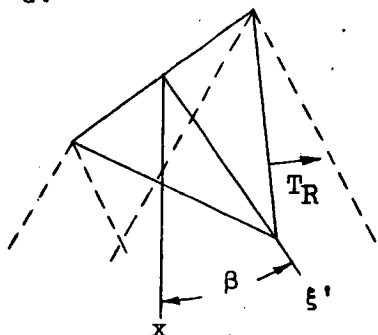
where

$$a = \frac{2c_r \sqrt{1+m^2}}{3}$$

and

$$T_L = \frac{8a^2 c_r^2 q m \sqrt{1+\tan^2 \beta} \sqrt{1+m^2} \sqrt{(1+m^2)(1+\tan^2 \beta) - (B^2+1)(m-\tan \beta)^2}}{\pi (1+m \tan \beta + Bm - B \tan \beta) (Bm + B \tan \beta + 1 - m \tan \beta)}$$

G.



$$N'_G = -T_R a + T_R \frac{\xi' c.g.}{\sqrt{1+m^2}}$$

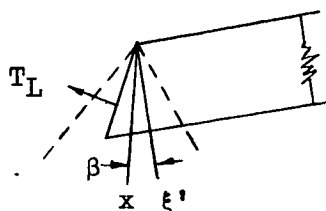
where

$$a = \frac{c_r(4+m^2)}{6 \sqrt{1+m^2}}$$

and

$$T_R = \frac{4q\alpha^2 c_r^2 \sqrt{1+m^2} \sqrt{1+\tan^2 \beta} \sqrt{(1+m^2)(1+\tan^2 \beta) - (1+B^2)(m+\tan \beta)^2}}{\pi (Bm+B \tan \beta + l - m \tan \beta) (B + \tan \beta)^2}$$

M.



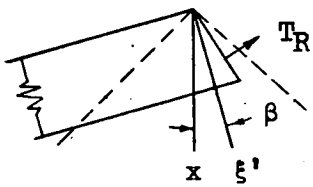
$$N'_M = T_L a - T_L \frac{\xi' c.g.}{\sqrt{1+m^2}}$$

where

$$a = \frac{3mb + 4c_r - 2c_r m^2}{6 \sqrt{1+m^2}}$$

and

$$T_L = \frac{4q\alpha^2 c_r^2 \sqrt{1+\tan^2 \beta} \sqrt{1+m^2} \sqrt{(1+m^2)(1+\tan^2 \beta) - (1+B^2)(m-\tan \beta)^2}}{\pi (l+m \tan \beta + Bm - B \tan \beta) (B - \tan \beta)^2}$$



$$N'_P = -T_R a + T_R \frac{\xi' c.g.}{\sqrt{1+m^2}}$$

where

$$T_R = \frac{4q\alpha^2 c_r^2 \sqrt{1+\tan^2 \beta} \sqrt{1+m^2} \sqrt{(1+m^2)(1+\tan^2 \beta) - (1+B^2)(m+\tan \beta)^2}}{\pi(Bm+B \tan \beta + 1 - m \tan \beta)(B + \tan \beta)}$$

for a raked-out tip, $m \geq 0$,

$$a = \left(\frac{3bm + 4c_r - 2c_r m^2}{6\sqrt{1+m^2}} \right)$$

and for a raked-in tip, $m < 0$,

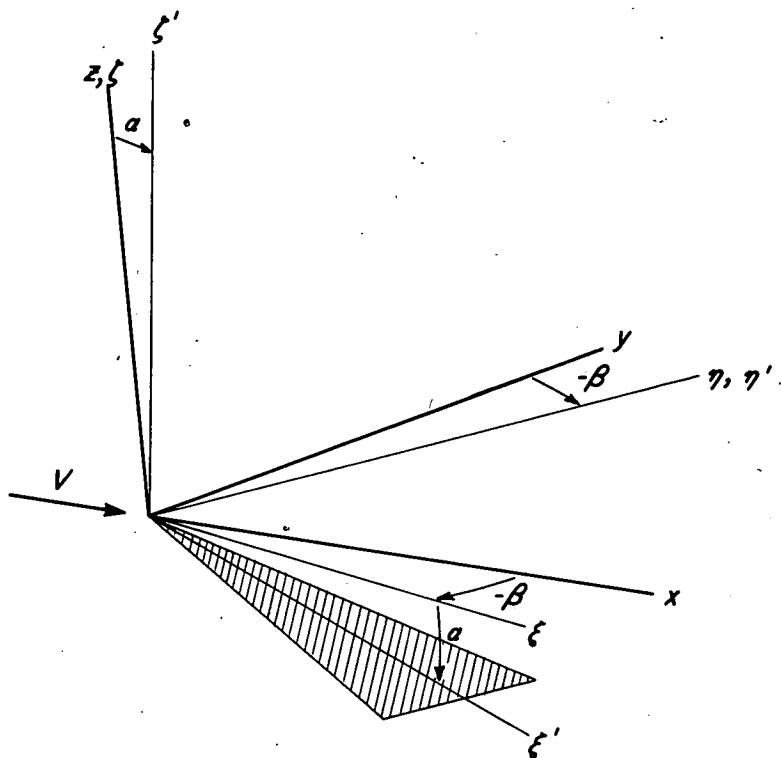
$$a = \frac{(3bm + 4c_r + 4c_r m^2)}{6\sqrt{1+m^2}}$$

REFERENCES

1. Jones, Arthur L., and Alksne, Alberta: The Damping Due to Roll of Triangular, Trapezoidal, and Related Plan Forms in Supersonic Flow. NACA TN No. 1548, 1948.
2. Jones, Arthur L., Spreiter, John R., and Alksne, Alberta: The Rolling Moment Due to Sideslip of Triangular, Trapezoidal, and Related Plan Forms in Supersonic Flow. NACA TN No. 1700, 1948.
3. Glauert, H.: A Non-Dimensional Form of the Stability Equations of an Aeroplane. R. & M. No. 1093, British A.R.C., 1927.
4. Ribner, Herbert S., and Malvestuto, Frank S., Jr.: Stability Derivatives of Triangular Wings at Supersonic Speeds. NACA TN No. 1572, 1948.
5. Malvestuto, Frank S., Jr., and Margolis, Kenneth: Theoretical Stability Derivatives of Thin Sweptback Wings Tapered to a Point with Sweptback or Sweptforward Trailing Edges for a Limited Range of Supersonic Speeds. NACA TN No. 1761, 1948.
6. Harmon, Sidney M.: Stability Derivatives of Thin Rectangular Wings at Supersonic Speeds. NACA TN No. 1706, 1948.
7. Jones, R. T.: Effects of Sweepback on Boundary Layer and Separation. NACA TN No. 1402, 1947.
8. Brown, Clinton E.: Theoretical Lift and Drag of Thin Triangular Wings at Supersonic Speeds. NACA TN No. 1183, 1946.
9. Puckett, A. E., and Stewart, H. J.: Aerodynamic Performance of Delta Wings at Supersonic Speeds. Jour. Aero. Sci., vol. 14, no. 10, Oct. 1947, pp. 567-578.
10. Robinson, A.: Airfoil Theory of a Flat Delta Wing at Supersonic Speeds. R.A.E. Rep. No. Aero 2151, A.R.C. 10222, 1946.

Page intentionally left blank

Page intentionally left blank



x, y, z rectangular coordinates of wind axes.

ξ, η, ζ rectangular coordinates of stability axes.

ξ', η', ζ' rectangular coordinates of body axes.



Figure 1.—Coordinate axis systems used in analysis.

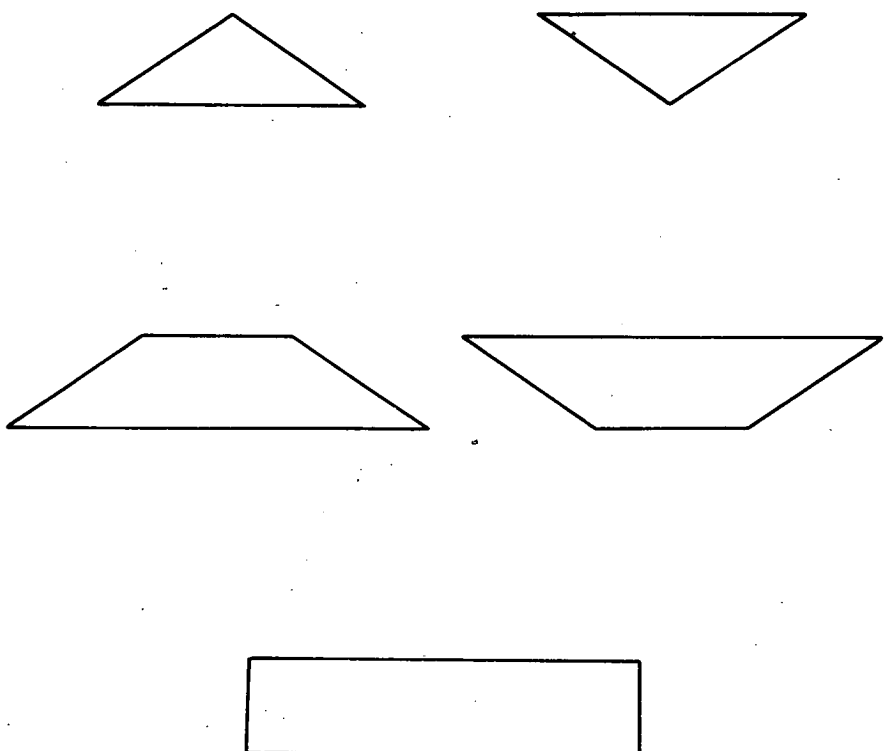


Figure 2.—The triangular, trapezoidal, and rectangular plan-form types investigated.

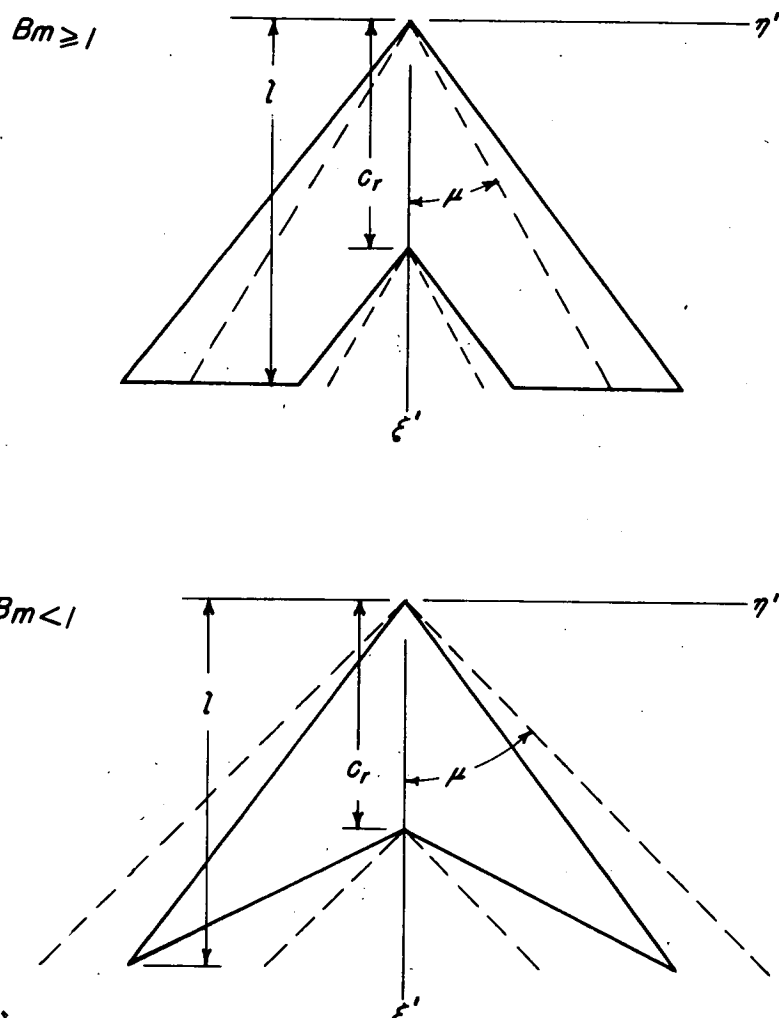


Figure 3.—Swept-back plan forms and Mach cone configurations investigated.

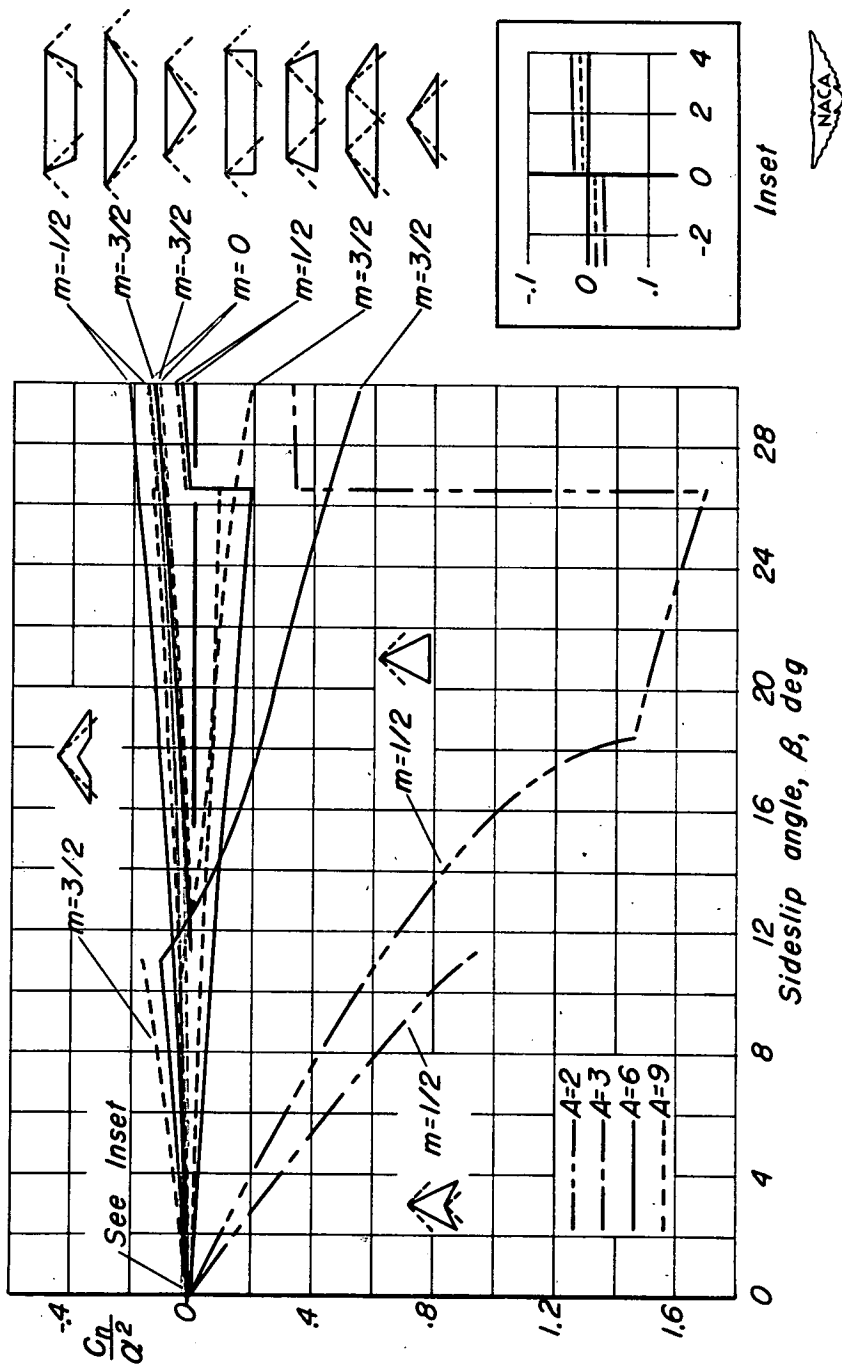


Figure 4.—Variation of yawing-moment coefficient squared with sideslip angle for $B=1$.

NACA

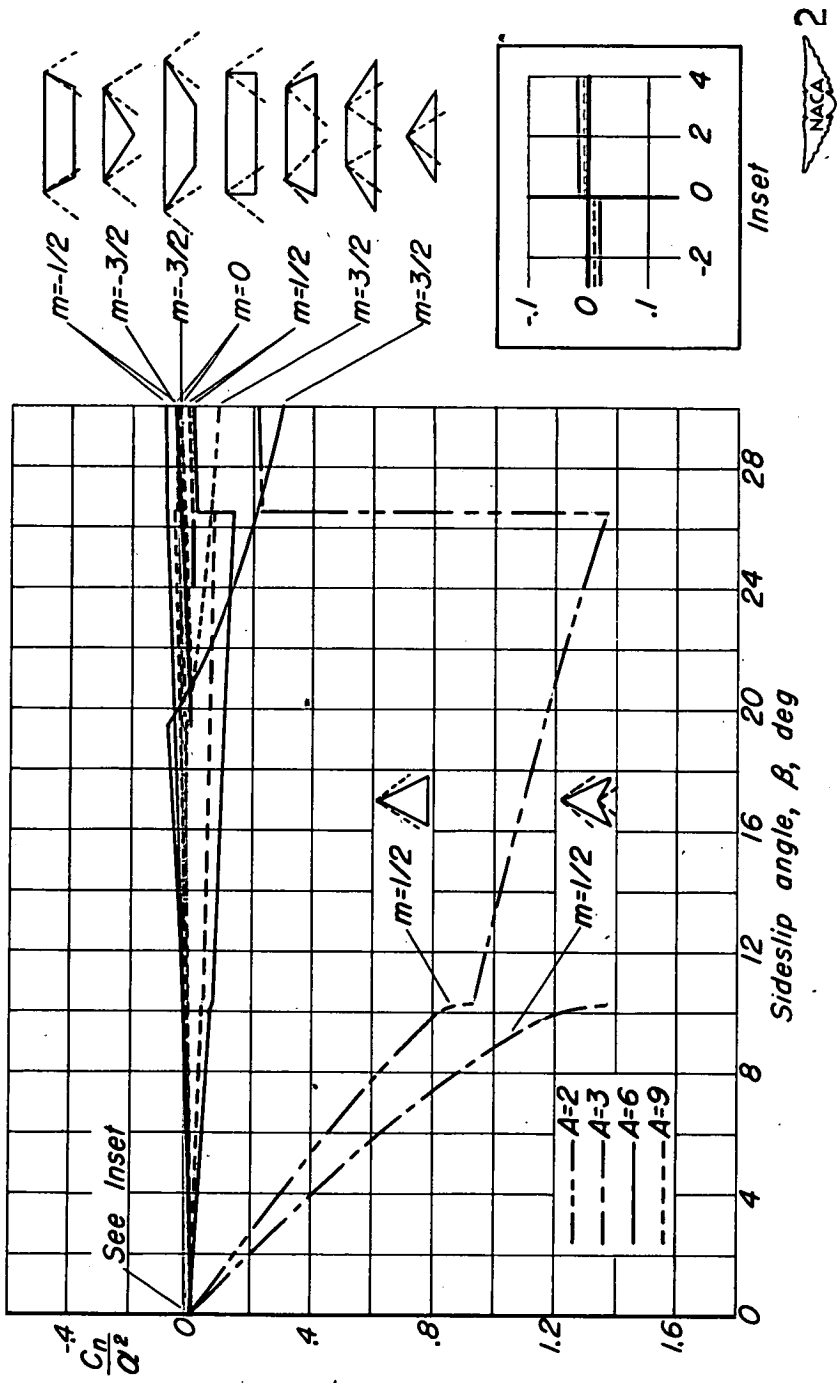


Figure 5.—Variation of yawing-moment coefficient per angle of attack squared with sideslip angle for $B=4/3$.

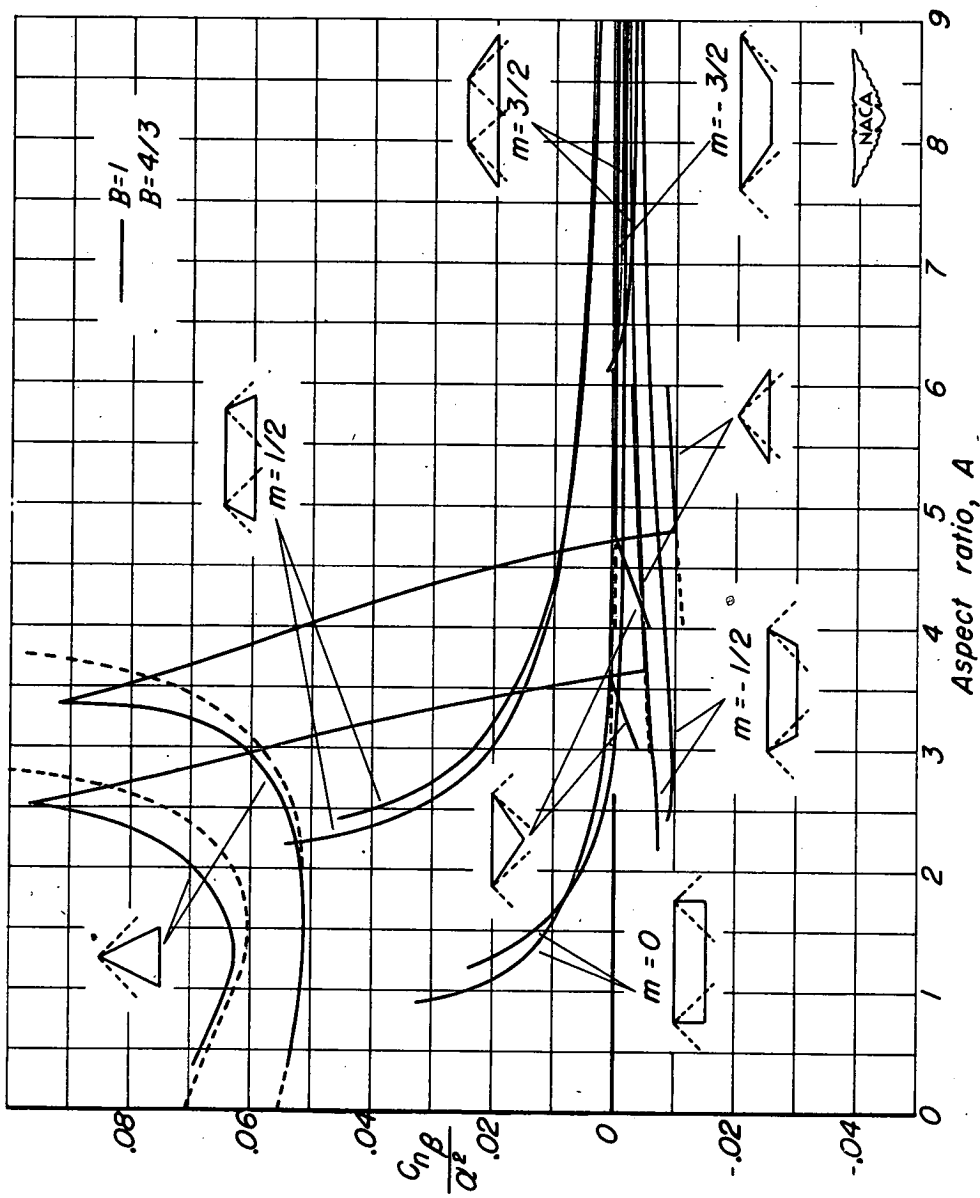


Figure 6.—Variation of yawing-moment-in-sideslip derivative per angle of attack squared with aspect ratio for typical triangular, trapezoidal, and rectangular plan forms; $B = 1$ and $B = 4/3$.

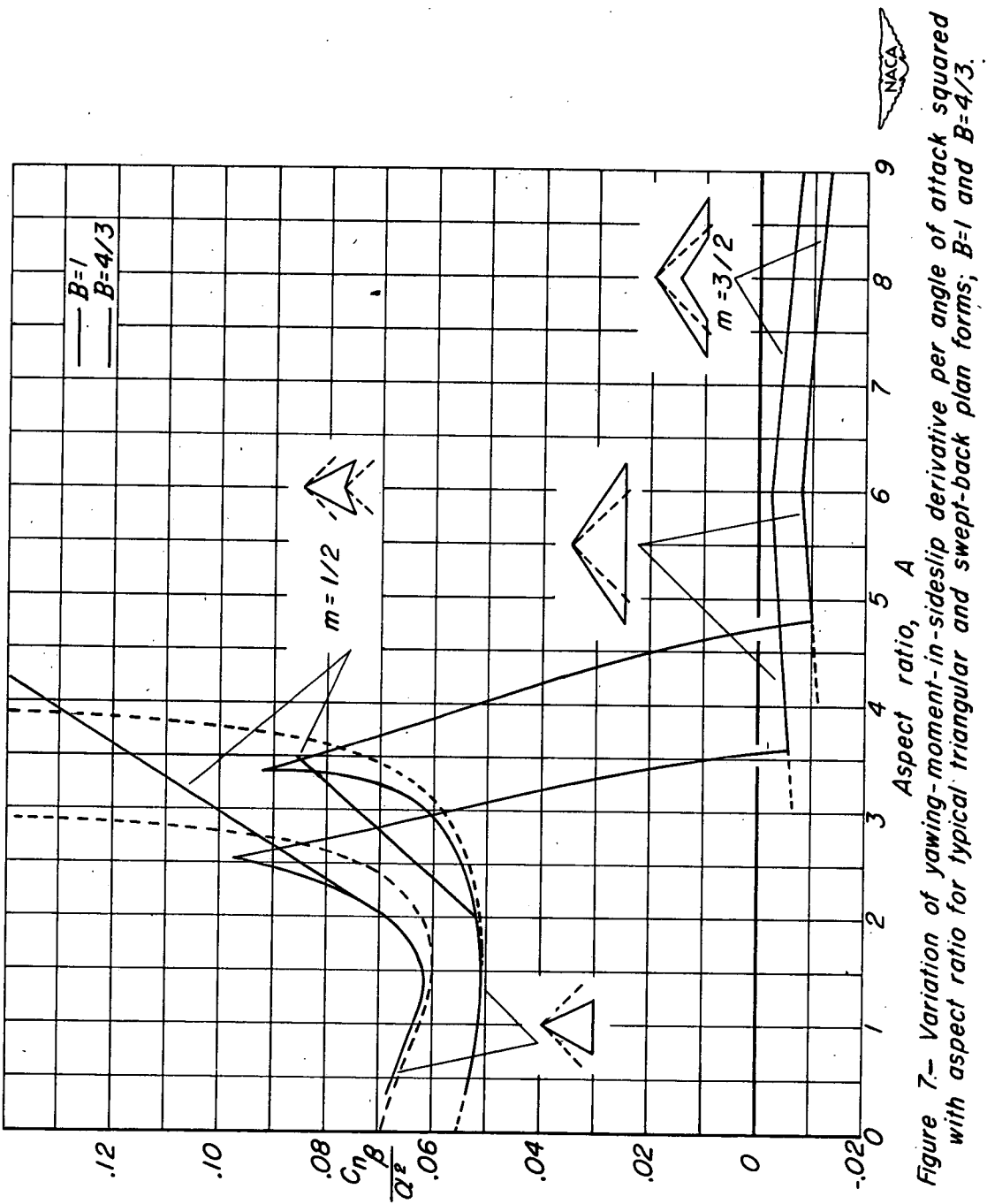
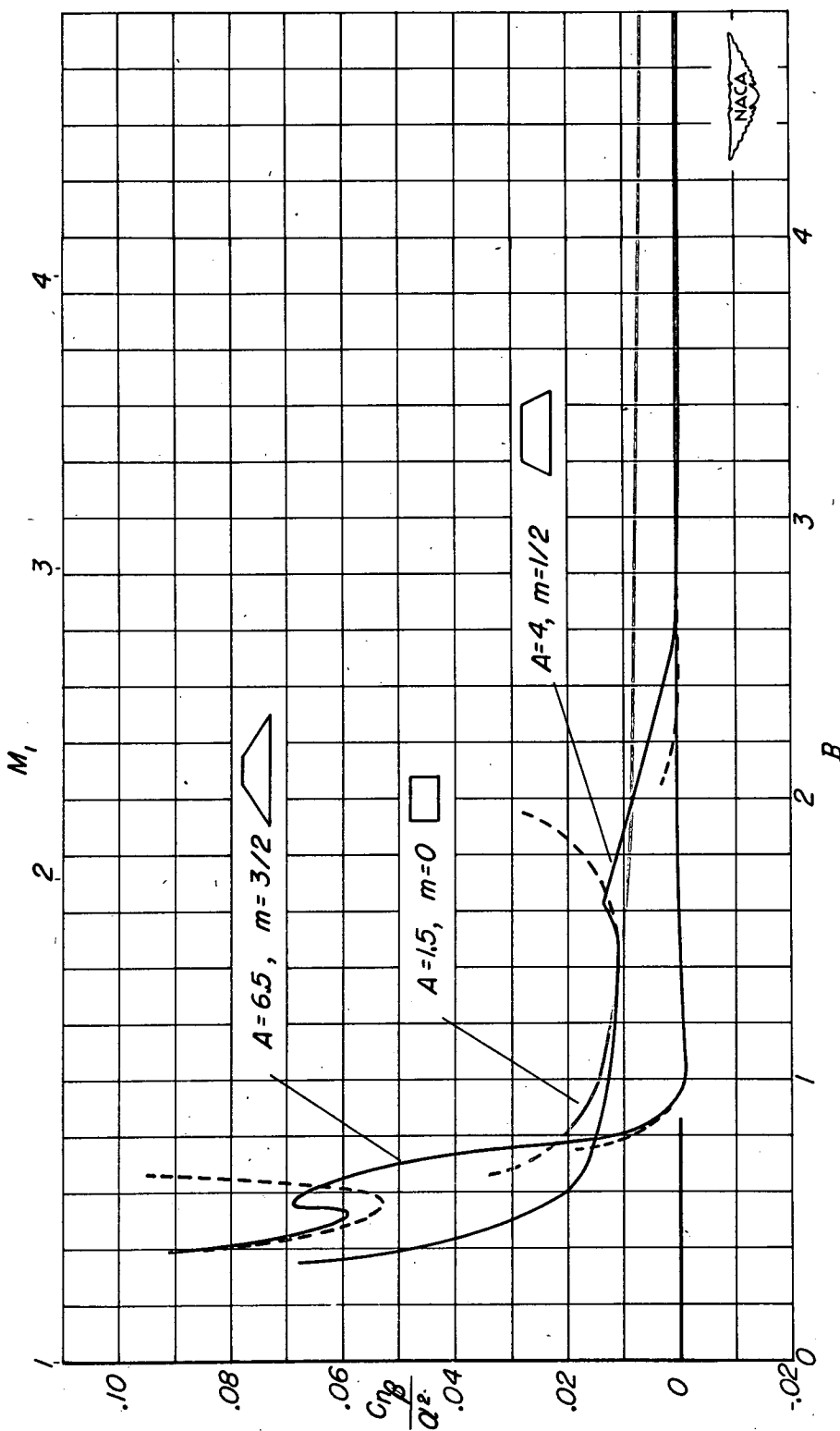


Figure 7.— Variation of yawing-moment-in-sideslip derivative per angle of attack squared with aspect ratio for typical plan forms; $B=1$ and $B=4/3$.



(a) Trapezoidal plan forms of aspect ratios 4 and 6.5 and rectangular plan form of aspect ratio 1.5.
Figure 8.- Variation of yawing-moment - in-sideslip derivative per angle of attack squared with Mach number parameter B .

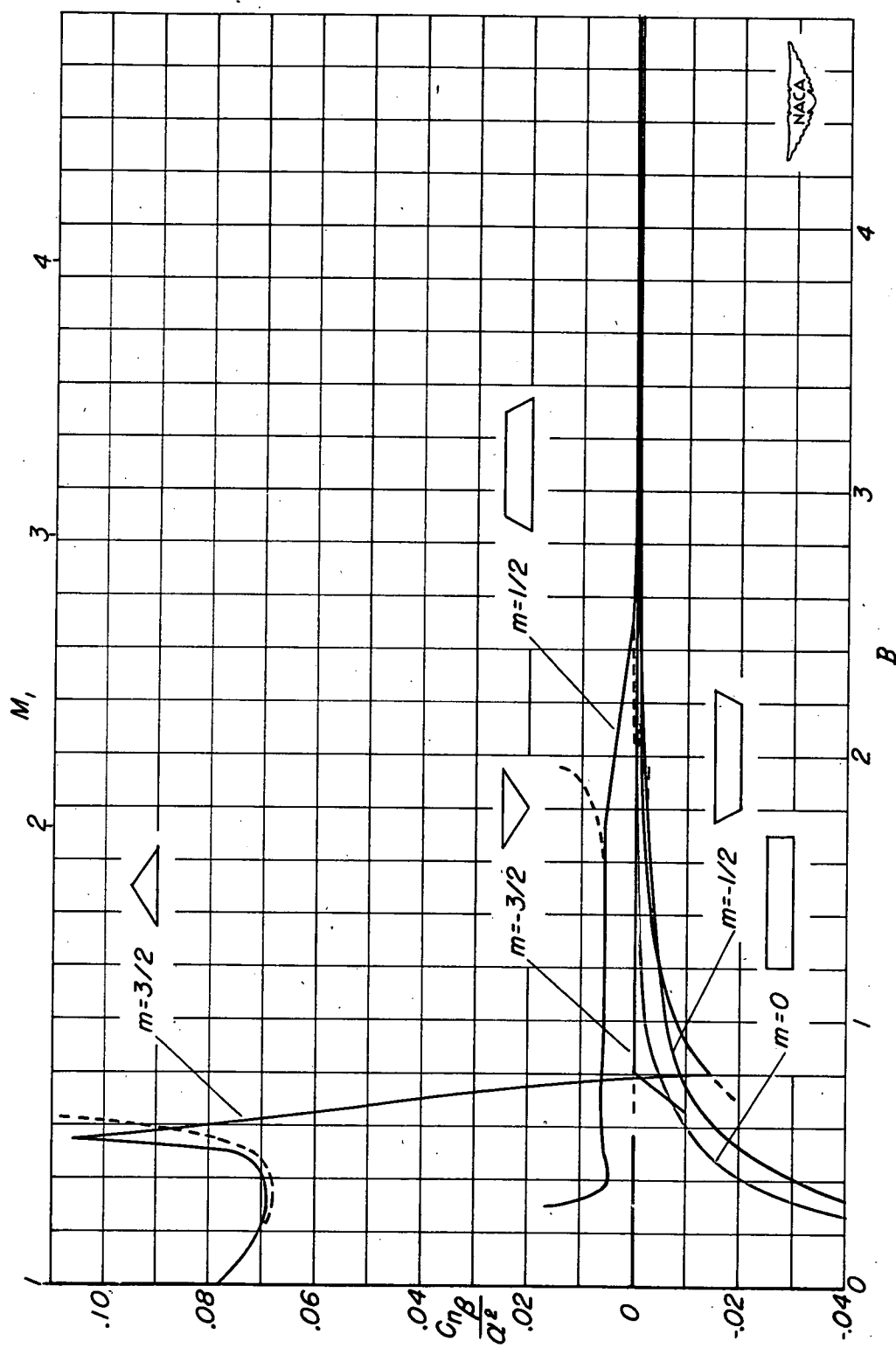


Figure 8.-Concluded.
(b) Triangular, trapezoidal, and rectangular plan forms of aspect ratio 6.

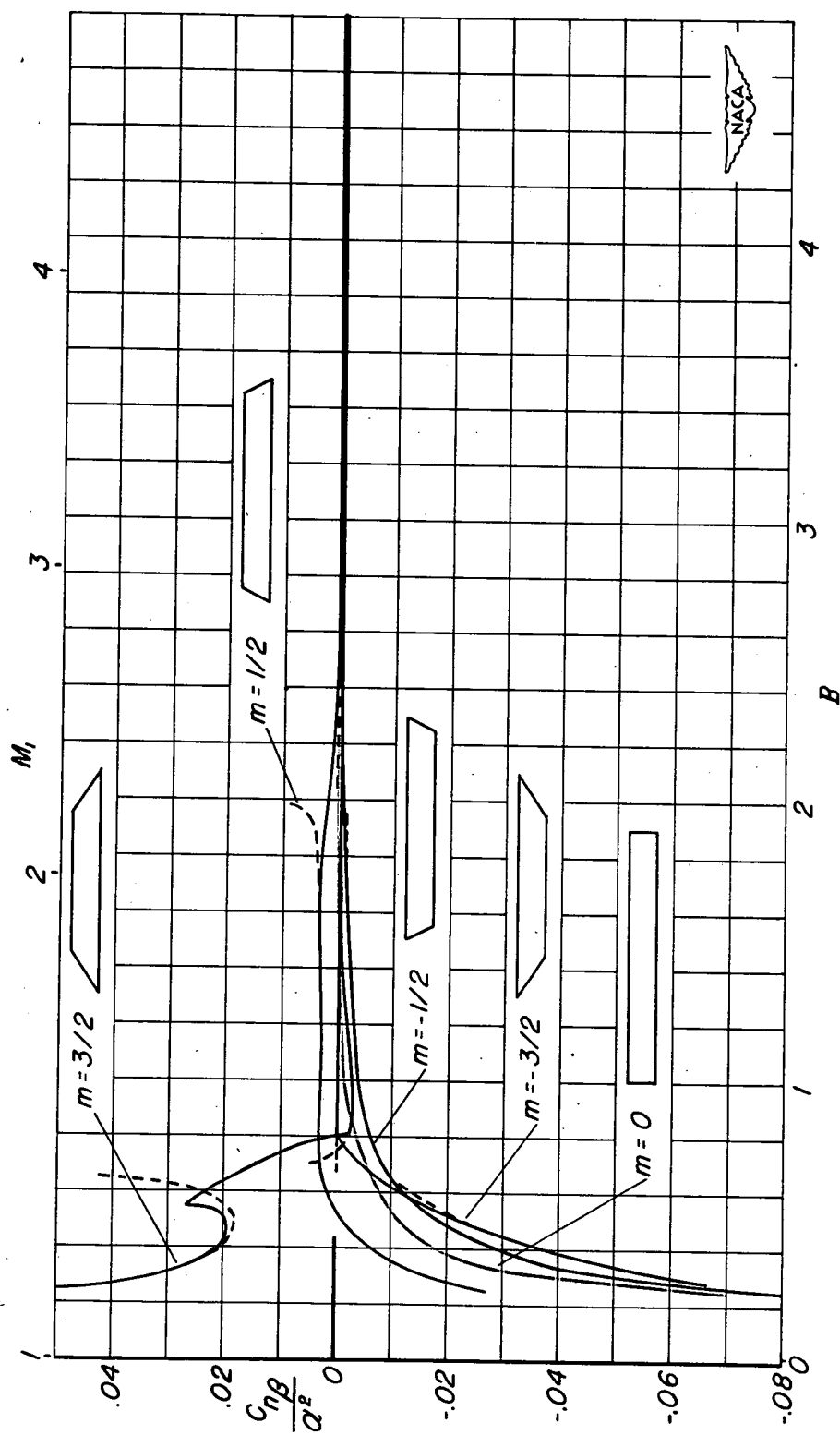


Figure 9.—Variation of yawing-moment-in-sideslip derivative per angle of attack squared with Mach number parameter B for typical trapezoidal and rectangular plan forms of aspect ratio 9.

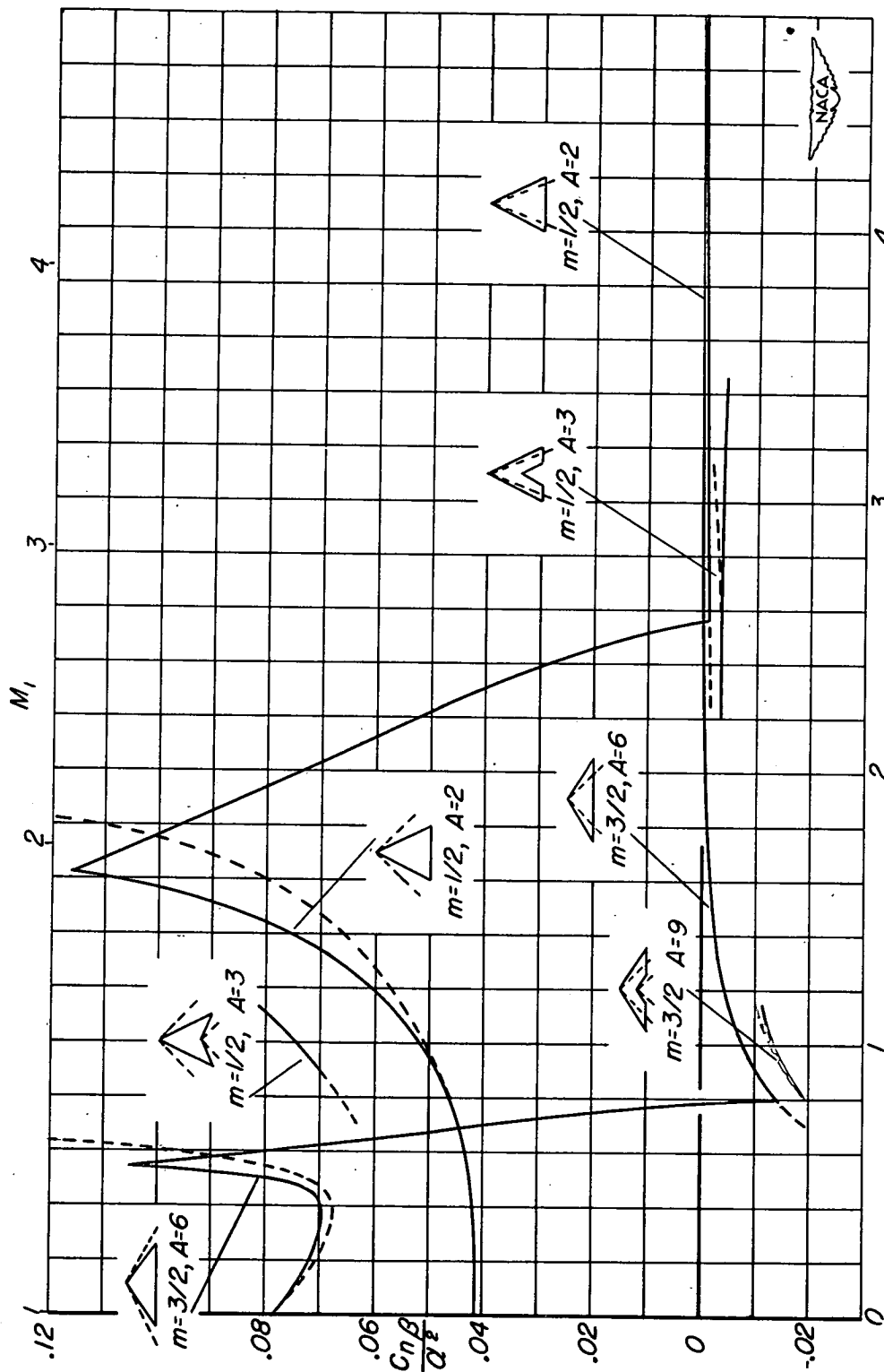


Figure 10.— Variation of yawing-moment-in-sideslip derivative per angle of attack squared with Mach number parameter B for typical plan forms.